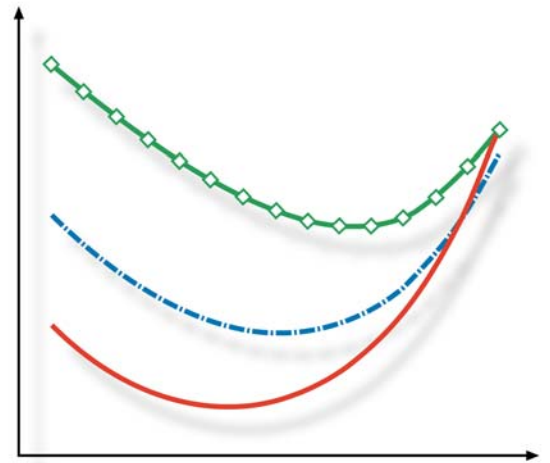
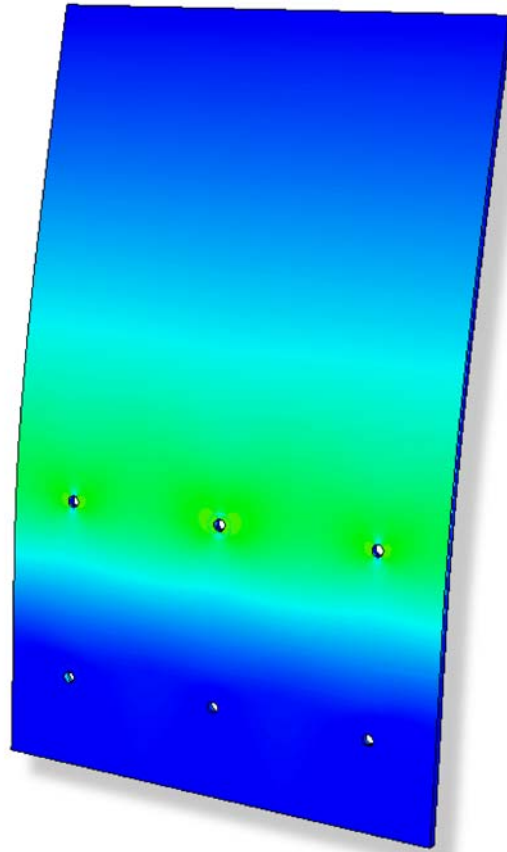




LUND
UNIVERSITY



STRENGTH DESIGN METHODS FOR LAMINATED GLASS

MARIA FRÖLING

Structural
Mechanics

Licentiate Dissertation

Department of Construction Sciences
Structural Mechanics

ISRN LUTVDG/TVSM--11/3071--SE (1-76)
ISSN 0281-6679

STRENGTH DESIGN METHODS FOR LAMINATED GLASS

MARIA FRÖLING

Copyright © 2011 by Structural Mechanics, LTH, Sweden.
Printed by Media-Tryck LU, Lund, Sweden, May, 2011 (*Pf*).

For information, address:
Division of Structural Mechanics, LTH, Lund University, Box 118, SE-221 00 Lund, Sweden.
Homepage: <http://www.byggmek.lth.se>

Acknowledgements

The work in this thesis has been performed at the Department of Construction Sciences, at Lund University. The financial support from the Swedish Research Council FORMAS, Glasbranschföreningen and Svensk Planglasförening is gratefully acknowledged.

I would like to thank my supervisors Anne Landin and Kent Persson for their guidance, support and encouragement. I owe gratitude to Kent Persson for his practical advice, help with technical details and fruitful feedback.

The reference group of this project is acknowledged for their interest in the project, support and advice.

Technical help from personnel at the center for scientific and technical computing at Lund University, LUNARC, is acknowledged. I would also like to thank Bo Zadig for help with graphical details. A thanks is directed to Johan Lorentzon for technical assistance.

I would like to thank the whole Department of Construction Sciences, and especially the Division of Structural Mechanics, for providing a supportive, open and creative work atmosphere.

Finally I thank my family and friends for support and friendship.

Abstract

In this thesis, methods for efficiently determining stresses in laminated glass structures are developed and tested. The laminated glass structures comprise both bolted and adhesive joints.

A recently developed finite element is suggested to be suitable for the modeling of laminated glass structures. The element is implemented and tested. It is proven by means of a simple test example that the element can be used in finite element analysis of laminated glass structures and give a good accuracy with a small fraction of the corresponding model size using standard solid elements. As an illustration of how the element would perform when more complicated glass structures are concerned, a similar element is implemented in the commercial finite element software ABAQUS and is used to analyze a laminated glass structure comprising one bolt fixing. The element performs well both when it comes to accuracy and efficiency. It is indicated that the new finite element is well suited for modeling laminated glass structures.

The new finite element is rigorously tested and compared to standard solid elements when it comes to the modeling of laminated glass structures. It is shown that the new finite element is superior to standard solid elements when it comes to modeling of laminated glass. The new element is applied to laminated glass structures comprising bolted and adhesive joints. Good results concerning accuracy and efficiency are obtained. The results show that the element may well be suited to model complex laminated glass structures with several bolted or adhesive joints.

The new element is used in the development of a method to compute stress concentration factors for laminated glass balustrades with 2+2 bolt fixings. The stress concentration factors are represented graphically in design charts. The use of the design charts allow the maximum principal stresses of the balustrade to be determined without using finite element analysis or advanced mathematics. The stresses can be computed for an arbitrary combination of geometry parameters of the balustrade.

It is illustrated how design charts for laminated glass balustrades with 3+3 bolt fixings are developed.

Keywords: finite element, computational techniques, laminated glass, stress concentration factor, design chart, bolt fixing, adhesive joint, balustrade.

Contents

1	Introduction	1
1.1	Background	1
1.2	Aim and Objectives	3
1.3	Limitations	3
2	Theory and Methods	3
2.1	The Material Glass	3
2.2	Types of Glass	4
2.2.1	Annealed Glass	5
2.2.2	Fully Tempered Glass	5
2.2.3	Heat Strengthened Glass	5
2.2.4	Laminated Glass	5
2.3	Mechanical Properties of Glass	5
2.4	Stress Prediction of Laminated Glass Structures	6
3	Related Research on Laminated Glass	8
3.1	Introduction	8
3.2	Experimental Results	8
3.3	Analytical Results	9
3.4	Numerical Results	11
3.5	Discussion	14
4	Stress Prediction of a Bolt Fixed Balustrade	14
4.1	General	14
4.2	Description of Example	15
4.3	Finite Element Analysis Using Three Dimensional Solid Elements	16
4.4	Finite Element Analysis Using M-RESS Elements	17
4.5	Stress Prediction Using Design Charts	17
4.6	Results and Comparison	19
5	Summary of the Papers	19
5.1	Paper1	19
5.2	Paper 2	19
5.3	Paper 3	20
6	Conclusions and Future Work	20

APPENDED PAPERS

Paper 1

Applying Solid-shell Elements to Laminated Glass Structures
Maria Fröling and Kent Persson

Paper 2

Computational Methods for Laminated Glass
Maria Fröling and Kent Persson

Paper 3

Designing Bolt Fixed Laminated Glass with Stress Concentration Factors
Maria Fröling and Kent Persson

1 Introduction

1.1 Background

During the past decades mass production of flat glass, development of new techniques to post-process the manufactured glass and the use of computational structural analyses by means of the finite element method have allowed for an increased use of glass as a structural material, [16]. Compared to other structural materials, for instance concrete, knowledge about mechanical properties and structural behaviour of glass is less. The result of this lack of knowledge has led to failure of several glass structures during the last years, [13].

In construction, the standard (elastic) design method is called the maximum stress approach, [16]. In the maximum stress approach, the engineer determines the dimensions of a structure through ensuring that the maximum stresses do not exceed the strength of the material at any position of the structure. The elastic design method is frequently used in glass structure design. When using the maximum stress approach, it is essential that the maximum stresses are predicted correctly. Only for standard geometries, boundary conditions and loading relatively simple methods based on formulas and design charts are available, [16].

One of the recent developments in the field of post-processing of glass is to laminate glass, [16]. Laminated glass normally consists of two or more layers of glass bonded with plastic interlayers. The most common material used for the interlayer is polyvinylbutyral (PVB). The use of laminated glass compared to single layered glass offers several advantages. When the glass breaks, the interlayer keeps the fractured glass together which increases safety. If one glass pane breaks the remaining layers can continue to carry the applied loads given that the structure is properly designed. Other advantages of laminated glass are their acoustic and thermal insulation properties. Due to the increased safety that is obtained, laminated glass is often used instead of single layered glass in structures.

Laminated glass displays a complicated structural mechanical behavior due to the combination of a stiff material (glass) and a soft material (PVB). Previous work, [21], shows that the discontinuous stress distributions that may develop in laminated glass panes subjected to certain loads and boundary conditions are difficult to model numerically. In Figure 1, a cantilever beam subject to bending by a point load at its right end is displayed. The beam is modeled by means of the finite element method using two dimensional plane stress elements in the xz -plane for both glass and PVB layers. The material parameters take on the values $E = 78$ GPa and $\nu = 0.23$ for glass and $E = 9$ MPa and $\nu = 0.43$ for PVB.

In Figure 2, the resulting distribution of normal stress in the thickness direction at a cross section located at the center of the beam is shown.

From Figure 2 it is evident that there are discontinuities in the levels of normal stress at the boundaries between the glass and PVB layers. Such discontinuities are normally most pronounced around holes and close to edges of a structure, [21]. It is common that the largest stresses occur in these regions ([7],[21]) and for the sake of safe design, it is important that the stress distributions are represented correctly by the model, particularly in these regions.

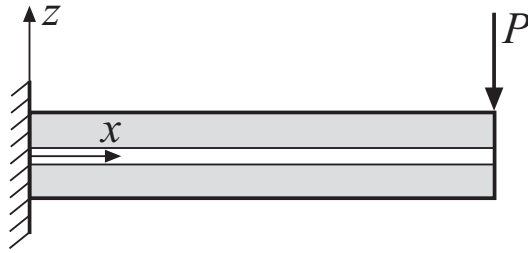


Figure 1: A cantilever laminated glass beam subjected to a point load.

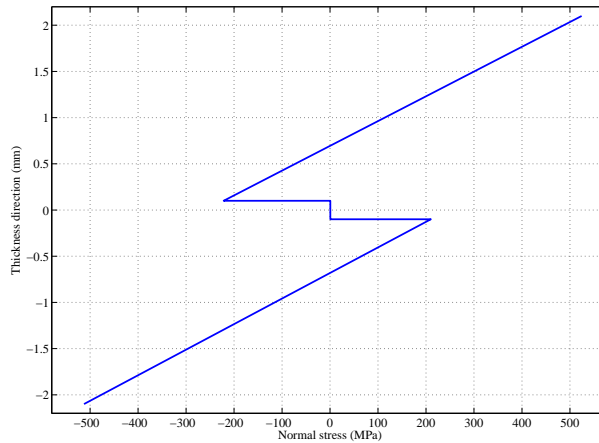


Figure 2: Distribution of normal stress along thickness.

Stress distributions as in Figure 2 are well captured by three dimensional solid elements. The disadvantage is that the resulting finite element models become very large which requires great computational effort. When modeling an engineering structure that comprises laminated glass panes, the computational time required may prevent fast and simple evaluation of different design alternatives. Papers 1 and 2 deal with the implementation of a new method for increasing the computational efficiency when modeling laminated glass structures by means of the finite element method.

In the design of glass structures, tables and graphs contained in design standards can be utilized when considering common geometries and boundary conditions. For more complicated geometries and boundary conditions, for instance bolt fixings, a detailed computational analysis is often required, [16]. The standard method for predicting the stress distribution in a laminated glass structure with several bolt fixings is to use three dimensional solid elements in finite element analyses. Very large finite element models are required for an accurate stress prediction of this type of structures, which makes the analyses practically impossible from a computational perspective. Using the method described in Papers 1 and 2, analyses are made possible, but decent knowledge about finite element analysis is required. The topic of Paper 3 is the development of design charts for bolt fixed laminated glass balustrades with a variable number of bolts. Thus, the design of

bolt fixed glass balustrades is made possible without performing advanced mathematics or finite element analyses.

1.2 Aim and Objectives

The aim of this thesis is to provide means of efficiently determining the stress distribution in advanced laminated glass structures. A recently developed finite element is implemented in finite element analysis and applied to laminated glass structures comprising structures that contain bolted and adhesive joints. The performance of the element in terms of accuracy and computational efficiency is tested and compared to conventional three dimensional solid element models. For bolt fixed laminated glass balustrades, design charts are developed for the determination of the stress distributions. The objective is to provide a relatively simple design tool for users that are less familiar with the finite element method.

1.3 Limitations

In the work developed in this thesis, some limitations are necessary. In the modeling of the bolts, only one type of bolt is used. It is a bolt for a cylindrical bore hole. Only one combination of thickness and material of the bush is considered. We also limit ourselves to stress predictions, leaving out details of further design work. When the design charts are developed, we restrict ourselves to the analysis of indoor balustrades, which somewhat simplifies the load situation since wind loads do not need to be considered, [9]. It is intended that the charts are not to be used for the highest line load (3 kN/m) according to Swedish construction standards, since for this case, a point load giving rise to a worst case loading situation is required in the analysis, [9]. Further, Swedish construction standards, [9], are used consistently when determining the load combination and balustrade height used in the analyses. It is assumed that the gravitational body force due to the weight of the structure could be neglected.

2 Theory and Methods

2.1 The Material Glass

Generally, glass forms when a liquid is cooled down in such a way that "freezing" happens instead of crystallization, [20]. Glasses do not consist of a geometrically regular network of crystals, but of an irregular network of silicon and oxygen atoms with alkaline parts in between, [16]. The most common oxide glass, silico-soda-lime glass, is used to produce glazing, [20]. Table 1 shows the chemical composition of silico-soda-lime glass according to European construction standards, [16].

When manufacturing glass, four primary operations can be identified: batching, melting, fining and forming, [20]. While the three first operations are used in all glass manufacturing processes, the forming and the subsequent post-process depend on which end product

Table 1: Chemical composition of silico-soda-lime glass (mass %).

Component	Chemical formula	Content (mass %)
Silica sand	SiO ₂	69-74
Lime (calcium oxide)	CaO	5-14
Soda	Na ₂ O	10-16
Magnesia	MgO	0-6
Alumina	Al ₂ O ₃	0-3
Others		0.5

that is manufactured. During the batching process, the correct mix of raw materials is selected based on chemistry, purity, uniformity and particle size, [20]. When melting the raw materials, glass furnaces are used. Different furnaces are used for producing different end products. The aim of the glass fining process is to produce a molten glass that is uniform in terms of composition and temperature and also bubble free.

Flat glass (which could be used for architectural glazing) is produced by the float process, which was introduced by Pilkington Brothers Ltd in the 1950s, [20]. It is noteworthy that this mass production process, together with continuously improved post-processes, have made glass cheap enough to allow it to be used extensively in the construction industry and to grow in importance as construction material during the past 50 years. Within the last two decades, further development within the field of post-processing operations, together with numerical analyses of structures (finite element analyses) have enabled glass to be used as structural elements in architectural glazing, [16]. In the start of the float process, the raw materials are melted in a furnace. Then, a fining process is used to eliminate bubbles. Later, the melt is poured onto a pool of molten tin, float, under a nitrogen atmosphere in order to prevent corrosion of the tin bath. Tin has higher specific weight (weight per unit volume) than glass, so that the glass floats on the tin. The glass spreads out and forms a smooth flat sheet at an equilibrium thickness of 6-7 mm. In order to produce various glass thicknesses, rollers working from the top of the glass are used. The speed of the rollers controls the glass thickness. The range of commercial glass thickness is 2-19 mm, [20]. During this phase, the glass is gradually cooled. The next step of the process is the annealing lehr, which slowly cools the glass in order to prevent that residual stresses are induced within the glass. After the lehr, the glass is inspected and it is ensured that visual defects and imperfections are removed. The glass is cut to a typical size of 3.21 × 6.00 m, [16], and then stored.

The standard flat glass produced through the float process is called annealed glass, [16]. Often further post-processing of the glass is required in order to produce glass products with different properties. For instance lamination of the glass and hole drilling are made at this stage.

2.2 Types of Glass

During the post-processing phase, glass types and products with different properties can be manufactured. Below, the most common glass types are described.

2.2.1 Annealed Glass

Annealed glass is standard float glass without further treatment. At breakage, annealed glass splits into large fragments, [16].

2.2.2 Fully Tempered Glass

Another commonly used term for fully tempered glass is toughened glass. During tempering, float glass is heated and then cooled rapidly (quenched) by cold air jets. The aim of the tempering process is to create a parabolic residual stress field that has tensile stresses in the core and compressive stresses at the surfaces of the glass. The surface of the glass always contains some cracks. Under a tensile stress field, the cracks are allowed to grow. If the glass is subjected to loads, cracks will not grow unless there is a net tensile stress field at the surface of the glass. Fully tempered glass usually breaks into small harmless pieces and therefore fully tempered glass is also termed safety glass, [16].

2.2.3 Heat Strengthened Glass

Heat strengthened glass is produced similarly as fully tempered glass, but the cooling rate is lower. The resulting residual stress is lower, and thus the tensile strength is lower than for fully tempered glass. At fracture, the fragments are larger than for fully tempered glass. On the other hand, the larger glass fragments allow for a greater post-breakage load capacity than for fully tempered glass, [16].

2.2.4 Laminated Glass

Laminated glass consists of two or more glass panes bonded by a plastic interlayer. The glass panes can have different thicknesses and heat treatments. Most common among the lamination processes is autoclaving, [16]. The use of laminated glass in architectural glazing is of great advantage for two reasons. Firstly, if one glass pane breaks, the remaining panes can continue to carry the applied loads given that the structure is properly designed. Secondly, the scattered glass pieces can stick to the interlayer and thereby serve to prevent people from getting injured. The interlayer is most often made of polyvinylbutyral, PVB. The nominal thickness of a single foil of PVB is 0.38 mm. It is common that two (0.76 mm) or four (1.52 mm) foils form one PVB interlayer, [16]. PVB is a viscoelastic material whose physical properties depend on the temperature and the load duration.

2.3 Mechanical Properties of Glass

Glass is an elastic, isotropic material and exhibits brittle fracture. In contrast to other construction materials, no plastic deformation occurs prior to failure. Therefore, local stress concentrations, occurring for instance close to bolt holes, are not reduced. The brittle characteristic of glass is of concern when constructing with glass as a load bearing element.

Glass has a very high theoretical tensile strength, up to 32 GPa is possible, [16]. However, the actual tensile strength depends on the influence of mechanical surface flaws. The compressive strength of glass is considerably higher than the tensile strength, since there is no surface flaw growth or failure under compression, [16].

In Table 2, relevant material properties of silico-soda-lime glass are summarized, [12].

Table 2: Material properties of silico-soda-lime glass.

Density	2500 kg/m ³
Young's modulus	70 GPa
Poisson's ratio	0.23

Table 3 summarizes strength values that could be used for structural design, [15].

Table 3: Strength values for glass design.

Compressive strength	880-930 MPa
Tensile strength	30-90 MPa
Bending strength	30-100 MPa

2.4 Stress Prediction of Laminated Glass Structures

When predicting stresses in laminated glass structures, there are two main options for stress predictions. The first possibility is to use formulas, tables or design charts. The other method consists of finite element analyses of the structure. The former method has the advantage that it is easy to use, but its use is limited to some general cases of geometry and boundary conditions, [16]. In this work, mainly bolt fixed connections are considered. For the case of bolt fixed laminated glass structures, finite element analyses must be used in most cases. In [16], an example of a design chart for a more advanced bolt fixed laminated glass structure is presented.

When making analyses using three dimensional solid elements, analysis results become sufficiently accurate given that the discretization of the model is fine enough. When analyzing the type of structures that are relevant in this work, finite element models become too large and the demand on computational resources too heavy. There is a scope for investigating alternative methods for performing finite element analyses of those structures. According to the classification of [24], laminated glass is a so-called laminated composite, which is made up of layers of different materials. For this category, there are several theories developed including corresponding numerical treatments. One means of reducing the model size is to use two dimensional models for composite plates, so-called Equivalent Single-layer Theories, (ESL), [24]. The two dimensional models are derived through making assumptions regarding the kinematics or the stress field in the thickness direction of the laminate in a fashion such that the three dimensional model is reduced to a two dimensional one. The simplest ESL theory is the Classical Laminated Plate Theory, (CLPT). It is an extension of the classical Kirchhoff plate theory to laminated composite

plates. In the CLPT theory, the assumptions regarding the displacement field are such that straight lines normal to the midsurface remain straight and normal to the midsurface after deformation. Thus, the transverse shear and transverse normal effects are neglected (plane stress). The First Order Shear Deformation Theory, (FSDT), extends the ESL theory through including a transverse shear deformation in the kinematic assumptions such that the transverse shear strain is assumed to be constant with respect to the thickness coordinate. In terms of kinematic assumptions this means that straight lines normal to the midsurface do not remain perpendicular to the midsurface after deformation. There are also higher order theories for laminated composite plates. The higher order theories may be able to more accurately describing the interlaminar stress distributions. On the other hand, they also require considerably more computational effort. In the Third Order Shear Deformation Theory, the assumption on straightness and normality of straight lines normal to the midsurface after deformation is relaxed. The result is a quadratic variation of the transverse stresses through each layer. Even higher order shear deformation theories are available, but the theories are complicated algebraically and expensive numerically, and yield a comparatively little gain in computational accuracy. The simple ESL laminate theories are often not capable of accurately determining the three dimensional stress field at ply level, which may be required for an accurate description of the stress distribution in a complex laminated glass structure.

An alternative is to use Layerwise Theories, [24]. The Layerwise Theories contain full three dimensional kinematics and constitutive relations. They also fulfill requirements on C_z^0 continuity, ([24], [11]). These requirements should necessarily be fulfilled in order to correctly describe the stress field in the thickness direction that characterizes laminated glass. Even if there are some computational advantages compared to full three dimensional element models, for instance that two dimensional finite elements could be used in the analysis, in the modeling of advanced structures the models may be computationally inefficient and difficult to implement, [24].

There exist several other layerwise models for laminated plates, see [24] and references therein. It is not the intention to provide a full review of various Layerwise Theories, so the interested reader is referred to the references provided in the reference cited above.

Another possible method, which is adopted in this work, is to use solid-shell elements. A solid-shell element is a three dimensional solid element which is modified so that shell like structures could be modeled in an appropriate manner. The basis for the solid-shell element used in this work, [10], is a conventional eight node three dimensional solid element. Since low-order three dimensional solid elements are used in order to model shell like structures, locking phenomena occur. In the solid-shell formulation, certain methods are incorporated such that locking is prevented. A review of solid-shell elements is provided in Paper 2. We note that through maintaining three dimensional constitutive relations and kinematic assumptions, the stress distribution of laminated glass can be accurately determined. The computational efficiency is increased due to the use of a special reduced integration scheme that only requires one integration point per material layer.

3 Related Research on Laminated Glass

3.1 Introduction

Past research on glass has focused mainly on monolithic (single-layered) glass, whereas the properties of laminated glass remain less well understood. The aim of this section is to review past research on the properties and behavior of laminated glass for architectural glazing. The review is subdivided into sections, where the first section deals with experimental testing, the second with analytical methods and the last section reviews numerical testing results. In the last section, emphasis is on Finite Element Method (FEM) analyses. It is shown that a clear cut division of previous research findings into these distinct categories is difficult, but the subdivision is rather a means of providing a structured presentation of the available knowledge.

3.2 Experimental Results

Most analyses on laminated glass units are experimental. This is particularly the case for plates, since the behavior is very complex, [1]. In this review we consider test results for both beams and plates. Studies on glass beams are often used to approximate the behavior of glass plates. According to Aşık, [1], this methodology is (generally) not acceptable, since the two structures have different stress and displacement fields.

One of the first studies on the behavior of architectural laminated glass subjected to structural loading is conducted by Hooper, [18]. In that study, the fundamental behavior of architectural laminates in bending is assessed. This is done by means of studies of laminated glass beams subjected to four-point bending. First, analytical formulas are derived for the shear force at the interface between glass and the interlayer and the central deflection respectively. These expressions are then used in combination with experimental bending tests in order to provide general understanding about the behavior of laminated glass beams subjected to bending as well as to produce data on interlayer shear stiffnesses (shear moduli) for various loading and temperature conditions. Results show that the bending resistance of the laminated glass is dependent upon the thickness and shear modulus of the interlayer. The physical properties of the interlayer are dependent upon the temperature and the duration of the loading. From an architectural designer's perspective, laminated glass which is subjected to sustained loads should be treated as consisting of two independent glass layers. For short-term loading, the bending stresses of the glass could be determined on the basis of an interlayer shear modulus corresponding to the maximum temperature at which such loading is likely to occur. When the glass is subjected to both sustained and short-term loading, the combined bending stress values in the glass layers may be calculated using the principle of superposition.

Behr et al., [3], reports on studies on the behavior of laminated glass units consisting of two glass plates with an interface of PVB. The glass units are subjected to lateral pressure (wind loads). Experiments are conducted in order to find out whether the behavior of a laminated glass unit is similar to that of a monolithic glass unit of the same thickness or to that of a layered glass unit consisting of two glass units and no interlayer. Results show

that the glass unit behaves more like a monolithic glass unit at room temperature. When temperatures are high, the behavior approaches that of two glass units without interlayer. Laminated glass units (two glass plates with a PVB interlayer) under uniform lateral loads and simply supported boundary conditions are investigated experimentally in Behr et al., [4]. According to the results, interlayer thickness effects on the structural behavior (in terms of corner stresses and center deflections) of laminated glass units are not large. Further, long-duration load tests at different temperatures are performed. For this case, the response in structural behavior is increasing as a function of time at load. Rates of increase in response in structural behavior decrease with time at load. In overview, the experimental data gathered during the tests are within theoretically derived monolithic and layered bounds on stresses and deflections.

Minor and Reznik, [22], study the failure behavior of laminated glass units. Three specimen sizes are used in the tests. Annealed monolithic glass samples are used as reference specimens. Laminated glass samples of the same dimensions and thicknesses as the reference specimens are tested to failure using the same loading rates as for the failure analysis of the reference specimens. Failure strengths are evaluated as functions of several variables: glass type (heat treatment), temperature and surface condition (subjected to surface damage or not). The most interesting result is that annealed laminated glass strengths are equal to annealed monolithic glass strengths at room temperature. This result is valid for all three sample sizes. Another interesting result is that when temperatures are increased, laminated glass strengths decrease.

Behr et al., [5], makes a reliability analysis of the glass strength data presented in [22]. The results of this analysis support the conclusions made in [22]. However, the reliability analyses suggest that the issue of the relative strength between monolithic glass units versus laminated glass units is complex at elevated temperatures. Whereas a clear strength reduction occurs in laminated glass at 77°C, little strength reduction occurs at 49°C. This indicates the possible existence of a break point in the relation between temperature and lateral pressure strength for laminated glass at around 49°C. Thus, for temperatures above this threshold it is suggested that the structural behavior of laminated glass is not longer similar to that of monolithic glass.

3.3 Analytical Results

Analytical work on laminated glass properties are scarce. In addition, most results are derived under various simplifying assumptions, [13].

In early work by for instance Vallabhan et al., [25], a previously developed computer model is used in order to analyze layered and monolithic rectangular glass plates subjected to uniform lateral pressure. The layered and monolithic plates have the same in-plane geometry total thickness. So-called strength-factors are developed for a variety of glass plate geometries. The strength-factor is defined as the ratio between maximum stresses in a monolithic plate and those in a layered plate. It is noteworthy that for certain geometries and loads, layered glass plates can possess larger maximum stresses than an equivalent monolithic glass plate. This result has an implication for the behavior of laminated glass plates, since a laminated glass plate is considered to display structural mechanical be-

behaviour in between the limiting cases of monolithic and layered plates. It is implied that the maximum stresses in a laminated glass plate can be close to (and even exceed) the maximum stresses in an equivalent monolithic glass plate under certain conditions.

Vallabhan et al., [26], use the principle of minimum potential energy and variational calculus, [17], in order to develop a mathematical model for the nonlinear analysis of laminated glass units. The final model consists of five nonlinear differential equations which are solved numerically and validated through full-scale experiments. The test specimens are square plates of laminated glass. The plates are simply supported and subjected to lateral pressure in increments. Stresses and corresponding principal stresses are calculated as a function of the lateral pressure. The results of the mathematical model compare very well with the experimental results. It is suggested that further research focuses on testing the mathematical model for various thicknesses of the laminated glass plates.

Norville et al., [23], set up an analytical beam model that explains data on deflection and stress for laminated glass beams under uniform load. The experimental data are presented in [6]. In the model, the PVB interlayer performs the functions of maintaining spacing between the glass sheets and transferring a fraction of the horizontal shear force between those sheets. The PVB interlayer increases the section modulus, i.e. the ratio between the bending moment at a cross section and the stress on the outer glass fiber at that cross section, of a laminated glass beam, and the magnitude of the flexural (bending) stresses in the outer glass fibers is therefore reduced. Thus, the strength of a laminated glass beam is higher than that of a monolithic glass beam with the same nominal thickness.

The analytical model of [26] is used in [1] in order to provide a set of graphs that shed light on the nonlinear behavior of simply supported, laminated glass plates typically used for architectural glazing. Such plates have very thin glass plies, which results in that they may undergo large deflections solely due to their own weights. This results in complex stress fields, which the author studies extensively. The result of the study is that the laminated glass plate that is studied undergoes very complex and nonlinear behavior when uniformly distributed load is applied. A conclusion is that nonlinear analysis is the only acceptable type of analysis for laminated glass plates.

In [2], a theoretical model for the behavior of laminated glass beams is presented. It is assumed that the glass beams are very thin such that large deflection behavior is used in the model building. The minimum potential energy and variational principles are used in the derivations. Three coupled nonlinear differential equations are obtained and closed form solutions are presented for simply supported laminated glass beams. The model is verified for the simply supported laminated glass beam through usage of experimental data and for a fixed supported laminated glass beam by means of finite element modeling. Also, the behavior of laminated glass is presented in comparison with the behaviors of monolithic and layered glass beams. Displacement, moment and stress functions for a simply supported laminated glass beam are given for the use in design to determine the strength of a laminated glass beam. It is proven analytically that the behavior of a simply supported laminated glass beam is linear even under large deflection. On the other hand, for the case of the fixed supported laminated glass beam, effects of membrane stresses are substantial and nonlinearities arise from geometric constraints. A discussion about the behavior of laminated glass beams versus laminated glass plates is conducted. It

is concluded that as earlier work on laminated glass plates show that simply supported glass plates undergo nonlinear behavior, simply supported laminated glass beams may not be used to draw conclusions about the behavior of laminated glass plates. In contrast, it is concluded that a study of nonlinear behavior of laminated glass beams makes sense concerning the behavior of laminated glass plates due to considerable similarities between these two cases.

Foraboschi, [13], sets up an analytical model for laminated glass beams under uniaxial bending. The model predicts stress developments and strength of laminated glass beams with given geometries, glass moduli of elasticity and PVB moduli of elasticity in shear. The ultimate load is determined using a design value of the glass tensile strength. The model is valid under the following assumptions: (i) plane cross sections in the whole beam, as well as in the PVB interlayer, do not remain plane and normal to the longitudinal axis (ii) glass is modeled in a linear elastic manner (iii) PVB is modeled in a linear elastic manner by means of the modulus of elasticity in shear, given that the value of this parameter is related to temperature and duration of loading. The latter assumptions allows a closed-form solution to the problem, contrary to the case when PVB is modeled in a viscoelastic manner. Since no particular simplifications are made when formulating the model, the model predictions are in excellent agreement with test results. In particular, no presumed strength-factor, [25], has been used in order to account for the contribution of the PVB layer to the bending capacity through its capacity to transfer horizontal shear force between the glass layers. An analysis of commercial-scale laminated glass beams is made in order to gain information regarding the rational design of laminated glass beams. Failure strengths and loads are determined for these cases. A comparison is made between the laminated glass model and monolithic and layered equivalency models respectively with respect to failure strengths and loads. Some of the major results are: 1) The greater the value of the shear modulus of elasticity of PVB and the thinner the PVB layer, the closer the prediction of the stress values are to those of the monolithic equivalency model and the greater is the tensile strength of the beam. 2) Irrespective of parameter values, the layered model is not suitable for analyzing laminated glass beams with the actual loads and boundary conditions. The conditions of the layered model is only approached as the temperature is reaching a value that prevails during fire exposure or similar conditions. 3) When the thickness of the beam is designed appropriately, the strength of the beam is raised by up to 70-80 %. 4) The historical assumption that the strength of laminated glass is equal to 60 % of the strength of monolithic glass of the same thickness is sufficiently preservative, but it doesn't represent a lower bound. The benefit of using the above relation is that it provides a simplification, but at the cost of the risk of underestimating the actual load-bearing capacity. 5) The behavior of the monolithic equivalency model is far away from that of a laminated glass beam, and the implementation of the model for design purposes is not recommended.

3.4 Numerical Results

A study of stress development and first cracking of glass-PVB (Butacite) laminates is performed in [8]. Fracture behavior is studied during loading in biaxial bending. A three

dimensional finite element model which incorporates the role of PVB thickness and the viscoelastic character of the PVB layer in stress development in the laminate is developed and tested. The finite element model is combined with a Weibull-description of glass strength in order to provide a failure prediction framework for the present set up. The glass is modeled using eight-node brick elements with incompatible modes for accurate capture of bending modes. The PVB layer is modeled using eight-node brick elements with incompatible modes using a hybrid formulation. The commercial finite element code ABAQUS is used in the investigations. Comparisons to experimental test data show that the finite element model is in good agreement. Stress development in the laminate is determined for a set of experimental loading rates. At a slower loading rate, each glass plate deforms nearly independently. At a faster loading rate, the overall stresses are higher for a certain deflection which indicates a higher overall stiffness. There is also a shift in the location and magnitude of the peak tensile stress of the laminate. This shift is expected to change the initiation of the first cracking, which is also shown in subsequent investigations. It is shown, both experimentally and through finite element modeling, that the peak stress changes locations with the loading rate. Two primary modes for the initiation of failure associated with changes in maximum stress are identified: (i) first crack located in the upper ply at the glass/PVB-surface and (ii) first crack located in the lower glass sheet at the outer glass surface. Regarding a comparison to the behavior of the corresponding monolithic and layered models, it is observed that at moderate loading rates, the stress in the laminate is higher than in the equivalent monolith. For the highest loading rates, the laminate demonstrates stress behavior similar to the monolith. Furthermore, it is shown that the peak stress locations is a complex function of loading rate, polymer thickness and load uniformity. The first-cracking sequence is affected by interlayer thickness and loading distribution: concentrated loading and thicker/softer interlayer gives first cracking in the upper ply and distributed loading and stiffer/thinner interlayer promote initial cracking in the lower glass sheet. The failure sequence is a function of loading rate and temperature: high temperatures and/or slow loading rates promotes first cracking in the upper ply whereas low temperatures and/or high loading rates lead to lower ply first cracking. The probability of first cracking can be computed by combining the finite element model with a Weibull statistical description of glass fracture. The approach used in this paper can form a foundation for laboratory tests for laminates and can be extended to encompass laminate plates used in commercial applications.

Van Duser et al., [27], present a model for stress analysis of glass/PVB laminates used as architectural glazing. The model consists of a three dimensional finite element model incorporating PVB viscoelasticity and large deformations. Studies are performed on a square, simply supported glass/PVB laminate subjected to uniform loading. The question of load-bearing capacity for first glass fracture of the plate is addressed through combining the finite element model with a statistical (Weibull) model for glass fracture. The approach used in this paper extends the work of Bennison et al., [8], to apply to commercial-scale architectural laminated glass plates, rather than laboratory scale disks. Results from the modeling exercise is compared to experimental results from [26]. The framework developed for stress analysis and failure prediction may be applied to laminates of arbitrary shape and size under specified loading conditions. Validated against

more extensive data the method may be used to develop new design standards for laminated glass. Regarding the finite element model, the glass sheets are modeled using 8-node solid elements with incompatible modes to avoid locking in bending. The PVB interlayer is modeled using eight-node solid elements with incompatible modes using a hybrid formulation in order to account for nearly incompressible deformations. The commercial program ABAQUS is used for the analysis. Accuracy of the finite element model is obtained through successively refining the mesh until mesh-independent results are obtained. The model predictions are in excellent agreement with data presented in [26]. One of the main findings of the study is that for most of the range of pressure used in the study, the probability of failure is lower than the monolithic limit, except at low pressures. At those pressures and stresses that would be used in design, laminate strength for this case would be predicted to be higher than for the equivalent monolithic glass plate. Since the concept of layered and monolithic limits is defined based on small strain analysis of beams, and doesn't take into account the membrane-dominated stress state that develops in large deflection of plates close to glass first cracking, a stress analysis that involves comparison to these limiting states could be misleading. In fact, if the derivation of these limits are based on transition to membrane-like behavior (large deflections), the stresses and deflections for a layered system in the membrane limit are exactly the same as for the equivalent monolithic plate. Since the monolithic limit ignores the thickness of the interlayer, the first cracking strength of the laminate may be larger than that of the monolith. Further, it is shown that stress development in the laminate is temperature (or loading rate) dependent. The influence of temperature can be diminished at large deflections as membrane stresses dominate and the coupling between the glass sheets play a lesser role in the stress development. Somewhat surprisingly, for typical glass Weibull moduli ($m \sim 5-10$) the probability of first cracking is only weakly dependent on temperature. The model of van Duser et al., [27], is based on a three dimensional finite element formulation. Thus, the resulting model becomes very large and the computations are expensive. This is noted by Ivanov, [19], who aims at investigating the effect of design parameters on the strength and stiffness of glass laminates. Another aim is to perform structural optimization of glass laminates. It is emphasized that both complicated analytical models that require numerical solutions and computationally expensive models are inappropriate for such analyses. The paper treats the case of a simply supported glass/PVB beam. The following simplifications are used: (i) only a plane beam is considered and (ii) the problem is confined to small strains and displacements. The representation of the laminated glass as a plane multilayer beam leads to a plane problem of theory of elasticity, which requires less equations although the same degree of discretization through the thickness of the beam and makes the corresponding finite element analysis more computationally efficient. The materials (glass and PVB) are both represented by linearly elastic material models. At the first stage of the analysis, a finite element model is developed. The model is used for the analysis of the case bending of a laminated glass beam under transverse forces. The beam is analysed by means of the finite element analysis software ANSYS 6.1. A linear finite element analysis is performed and yields data on nodal deflections, strains and stresses. The analysis shows that the bending stress in the glass layers is determinant for the load-bearing capability of laminated glasses, but the shear in the PVB layer is

important for glass-layer interaction. Based on this first analysis step an analytical model of a laminated glass beam is developed. The model is based on Bernoulli-Euler beam theory for each glass layer, with an additional differential equation for the PVB interlayer shear interaction. The obtained differential equations are easily solved analytically for the case of a simply supported beam under uniform transverse load. The mathematical model is validated against the previously developed two dimensional finite element model and against analytical results from [2]. For both cases, the results of the analytical model show great agreement with other solutions. The model is used to perform a parametric study of the influence of layer thicknesses on deflections and stresses of a beam under transverse uniform load. Later, the model is utilized for lightweight structure optimization of layer thicknesses. The results show that the inner layer of laminated glasses could be thinner than the external glass layer and that the optimally designed laminated glasses could be superior to monolithic glasses in all criteria.

3.5 Discussion

To summarize the review above, one can conclude that most of the investigations done consider beams and plates of regular geometries subjected to standard point loads or uniformly distributed loads. Some attention is directed towards the physical properties of the interlayer. A main issue is to place laminated glass structural behavior correctly in relation to the behavior of layered and monolithic equivalency models for different geometries and loading cases. Some investigations deal with the fracture behaviour of simple structures. Analytical models of various complexity have been developed in order to describe the structural mechanic behaviour of laminated glass beams. Finite element models are mainly three dimensional and are developed for the purpose of investigating failure behaviour or for optimization purposes. In all cases the structures are simple (beams and plates) and the boundary conditions are standard. One author mentions that model size constitutes a limitation when it comes to analyzing laminated glass beams subjected to uniaxial bending for optimization purposes. The remedy is to use a plane (two dimensional) finite element model rather than a full (three dimensional) model.

4 Stress Prediction of a Bolt Fixed Balustrade

4.1 General

In this section an example of a glass structure with bolted joints is used in order to demonstrate the use of the two stress prediction methods presented in this thesis. The example comprises a laminated glass balustrade of the type presented in Paper 3. Since the balustrade in this example has 3+3 bolts, it is simultaneously shown how the concept of design charts can be expanded to balustrades with the increased number of bolts. The results in terms of accuracy are compared to results that are obtained when a standard finite element method is used.

4.2 Description of Example

The structure is a balustrade of laminated glass consisting of two glass layers with an intermediate PVB layer. The structure contains 3+3 bolt connections, which means that this example is also used to illustrate how design charts was developed for the case of 3+3 bolt connections. In Figure 3, the two dimensional geometry of the structure is displayed.

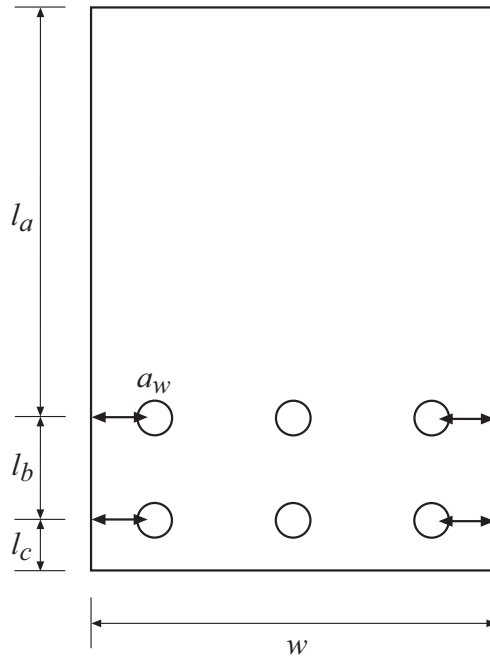


Figure 3: Two dimensional geometry of balustrade.

Cylindrical bolts with bolt head diameter, d_b , of 60 mm were used. The bolts are made of steel and have bushes of EPDM at the contact surfaces with the glass. The bore hole diameter, d_h , was set to 22 mm. A list of the geometry parameters with corresponding design values is included in Table 4. t_{PVB} is the thickness of the PVB layer, t_{EPDM} is the thickness of the EPDM layer and t_g is the glass thickness.

As an example, a horizontal (uniform) line load was applied at the upper edge of the glass balustrade. The load had the magnitude 3 kN/m. All materials were modeled as isotropic and linear elastic materials. In Table 5, the material parameter values are presented. E denotes modulus of elasticity and ν denotes Poisson's ratio for glass, PVB, EPDM and steel respectively.

In the coming subsections, it is described how the test example was analysed using three different methods. First, three dimensional solid elements were used in ABAQUS in order to provide a benchmark solution to which the two other methods were compared. Then, M-RESS elements were used in ABAQUS in order to illustrate the applicability of the method presented in Papers 1-2 to this test problem. Finally, design charts for balustrades with 3+3 bolt connections are introduced and it is shown how the charts were used in order to analyze the balustrade. Design charts for balustrades with 2+2 bolt connections

Table 4: Design parameters for test example.

l_a	1.275 m
l_b	0.48 m
l_c	0.24 m
a_w	0.18 m
w	1.23 m
t_{PVB}	0.76 mm
t_{EPDM}	3 mm
d_h	22 mm
d_b	60 mm
t_g	12 mm

Table 5: Material parameters for test example.

E_g	70 GPa
ν_g	0.25
E_{PVB}	6.3 MPa
ν_{PVB}	0.4
E_{EPDM}	20 MPa
ν_{EPDM}	0.45
E_s	210 GPa
ν_s	0.3

is the topic of Paper 3.

4.3 Finite Element Analysis Using Three Dimensional Solid Elements

In this subsection, second order three dimensional solid elements were used in ABAQUS in order to provide a benchmark solution to the problem presented in the former subsection. For each bolt, the entire bolt head consisting of a steel part and an EPDM layer was explicitly modeled. Only those bolts located at positions where equilibrium reaction forces acting on the glass occur, were included in the model. Constraints of the type tie were used between the glass pane and the EPDM layers. As boundary condition it was used that displacements are prohibited in all directions at the opposite side of the bolts. Second order three dimensional solid elements (C3D20R) were used for the glass and PVB layers. Standard linear three dimensional solid elements (C3D8R) were used for the other parts of the model. A total of about 270000 elements were used. The line load was converted to a pressure load acting on al surface of infinitely small width, since it is not possible to apply line loads in ABAQUS. The maximum principal stress occurred at the middle bolt of the upper bolt row, as is indicated in Figure 4, and took on the value 119.4 MPa.

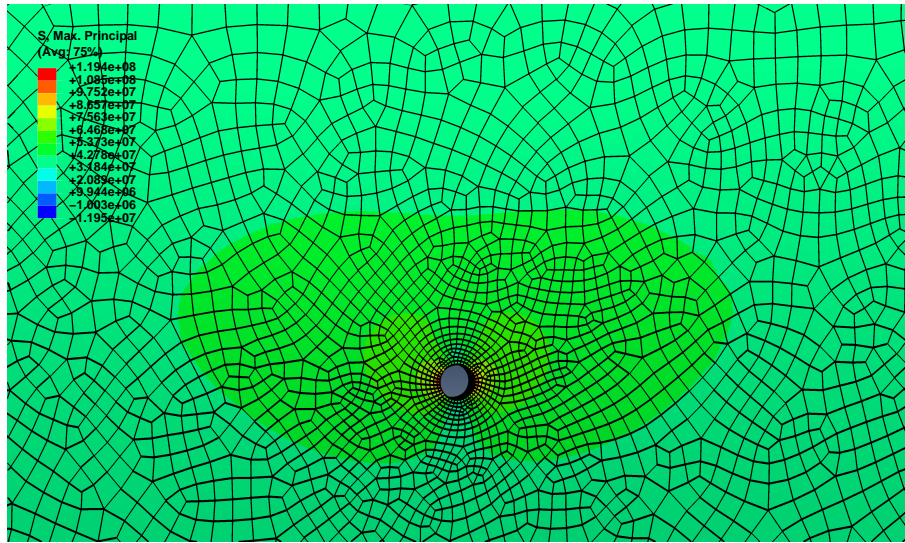


Figure 4: Maximum principal stresses for balustrade using three dimensional solid elements.

4.4 Finite Element Analysis Using M-RESS Elements

In this subsection, the model of the previous subsection was used, but the element type of the laminated glass was selected to be M-RESS. A modification of the model of the former subsection was necessary. The line load was distributed to nine equidistant points and applied as concentrated forces using manual lumping. In this model, two element layers per glass layer and one element layer for the PVB layer were used. In total, around 160000 elements were used. The maximum principal stress of the glass balustrade reached 125.5 MPa.

4.5 Stress Prediction Using Design Charts

In the course of writing this section, design charts for balustrades with 3+3 bolt connections were developed. The in-plane geometry of the balustrade is that of Figure 3. When comparing to the case of a balustrade with 2+2 bolt connections, the set of unknown parameters is the same. The development of the new design charts is thus a simple extension of the already developed charts. Table 6 displays the design parameters and the ranges of variation for each parameter.

In Figure 5, the design chart that applies to the test example of this section is displayed. Next, it is illustrated how the maximum principal stress of a glass balustrade with geometry parameters according to Table 6 and material parameters according to Table 5 was computed. First, the nominal stress value, σ_{Nom} , was computed using equations (1), (35), (37) and (39) of Paper 3.

Equation (1) gave $R_2 = 3000 \cdot 1.23 \cdot \left(1 + \frac{1.275}{0.48}\right) \approx 1.3492 \cdot 10^4$ N.

From equation (1): $M(0.48) = \frac{(1.3492 \cdot 10^4) \cdot 1.275 \cdot 0.48}{(1.275 + 0.48)} \approx 4.7049 \cdot 10^3$ Nm.

Table 6: List of geometry parameters.

Parameter	Value
l_a	1.25 m
l_c	0.24 m
t_{PVB}	0.76 mm
t_{EPDM}	3 mm
l_b	0.2, 0.4, 0.8 m
a_w	$0.1 - (\frac{w}{2} - 0.15)$ m in step of 0.025
w	0.9-2.7 m in step of 0.3 m
d_h	15-40 mm in step of 5 mm
t_g	6, 8, 10, 12 mm
d_b	60 mm

Equation (19) gave (using Matlab): $N(0.48) \approx -1.8008 \cdot 10^5$ N.

Equation (20) yielded $M(0.48) = \frac{1}{2}(4.7049 \cdot 10^3 + 0.012 \cdot (-1.8008 \cdot 10^5)) \approx 1.2720 \cdot 10^3$ Nm.

Finally, equation (21) gave $\sigma_{Nom} = \frac{1.2720 \cdot 10^3}{\frac{1.23 \cdot 0.012^2}{6}} - \frac{(-1.8008 \cdot 10^5)}{1.23 \cdot 0.012} \approx 55.3$ MPa.

In Figure 5, the applicable design chart for this case is displayed. The chart was selected as the one which has parameter values closest to the actual design example.

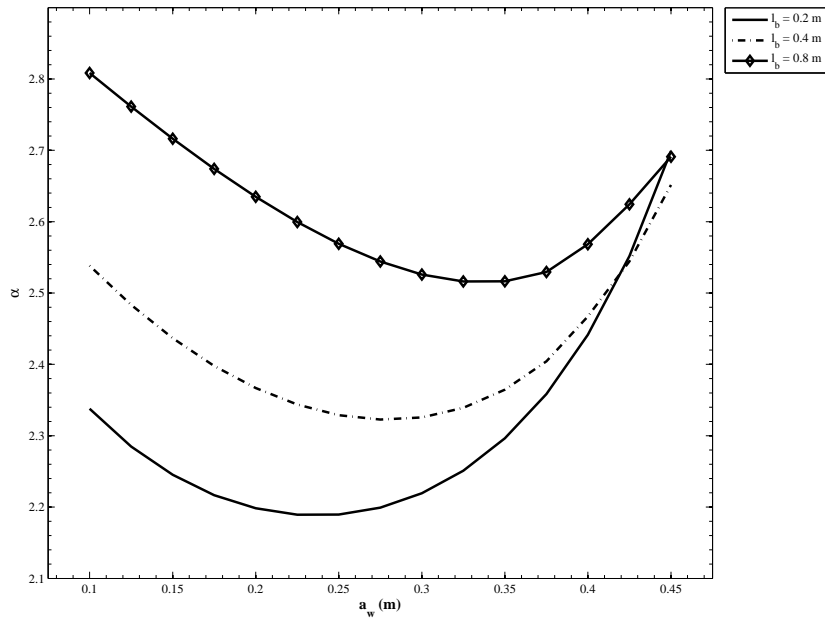


Figure 5: Design chart for $t_g = 12$ mm, $w = 1.2$ m, $d_b = 60$ mm and $d_h = 20$ mm.

In the diagram, $a_w = 0.18$ m was chosen on the x-axis, whereas in the case of l_b one had to interpolate between the isolines corresponding to $l_b = 0.4$ m and $l_b = 0.8$ m. The value of α which corresponded to the actual combination of parameters a_w and l_b , was

read off from the diagram, which yielded $\alpha \approx 2.44$. The maximum principal stress of the balustrade was determined according to $\sigma = \alpha \cdot \sigma_{Nom} = 2.44 \cdot 55.3 \approx 134.9$ MPa.

4.6 Results and Comparison

This subsection is devoted to a discussion and comparison of the results obtained using the various design methods discussed in this section. In Table 7, the values of maximum principal stress are presented. From the table one can conclude that the results are sufficiently

Table 7: Comparison of different methods for stress prediction.

Method	Maximum principal stress (MPa)
FEM, solid elements	119.4
FEM, M-RESS	125.5
Design chart	134.9

close to each other in order to classify the methods as yielding equivalent results. More rigorous comparisons of the two first methods are provided in Papers 1-2. The result using the third method carries some uncertainties related to mesh density when constructing the chart, the selection of the design chart to match the actual set of parameters, parameter interpolation and reading off the chart.

5 Summary of the Papers

5.1 Paper1

M. Fröling and K. Persson. Applying Solid-shell Elements to Laminated Glass Structures. Published in: *Glass Worldwide*, Issue 31, Sept/Oct 2010, 144-146.

Summary: Solid-shell finite elements are proposed by Maria Fröling and Kent Persson for the efficient and accurate modeling of laminated glass structures. The elements are applied to two test examples and performance is compared to 3D elasticity theory. One example involves a real world structure, where special attention is directed to the prediction of stress distribution around point fixings.

5.2 Paper 2

M. Fröling and K. Persson. Computational Methods for Laminated Glass. Submitted to: *International Journal of Applied Glass Science*.

Summary: A new solid-shell finite element is proposed for the purpose of efficient and accurate modeling of laminated glass structures. The element is applied to two test examples and the performance concerning accuracy and efficiency is compared to standard three dimensional solid elements. Further examples illustrate how the element could be applied in the modeling of laminated glass structures with bolted and adhesive joints.

5.3 Paper 3

M. Fröling and K. Persson. Designing Bolt Fixed Laminated Glass with Stress Concentration Factors. Submitted to: *International Journal of Applied Glass Science*.

Summary: A method for determining stress concentration factors for laminated glass balustrades with 2+2 bolt fixings is developed. The stress concentration factors are presented graphically in design charts. Through the use of simple formulas and the design charts, the maximum principal stresses of the balustrade can be determined for an arbitrary combination of the geometry parameters involved.

6 Conclusions and Future Work

This thesis deals with the development of methods for stress prediction of bolt fixed laminated glass structures. On one hand, a recently developed finite element, [10], is implemented and it is proven that the performance is accurate when it comes to the modeling of thin laminated glass structures subjected to bending as well as for laminated glass with bolted and adhesive joints. The computational performance is strongly improved compared to when a standard three dimensional solid element is used. One can conclude that this element could be used in finite element analyses of complex laminated glass structures with many bolt fixings or adhesive joints. On the other hand, a method is developed such that the maximum principal stress of a laminated glass balustrade with 2+2 bolt fixings could be determined using simple formulas and design charts. This leads to great time savings for the designer, since an investigation of the stresses of balustrades with different design parameters could be performed without finite element analyses. It is also not necessary for the designer to possess the advanced knowledge of the finite element method which is required in order to analyse advanced glass structures.

For future work, a number of extensions can be made when it comes to the development of the design charts. The most obvious extension is to develop similar charts for balustrades with 3+3 bolt fixings. The development of these charts is to a great deal finished, which has been demonstrated in Section 4. There are possibilities for developing charts for parameter combinations that have not been taken into account, for instance considering different thicknesses of the PVB layer. Other materials for the interlayer could also be considered. It could also be interesting to consider other types of bolts and bolts for countersunk holes. It is of course of interest to make sure that the design charts are in line with current Eurocodes, since Eurocodes substitute Swedish construction standards from the beginning of year 2011. An extension to include outdoor balustrades would also be within reach. Less obvious is to consider other types of connections, see [16] for an overview of different types of connections. Especially adhesive connections are of interest, because the larger contact area between the connection and the glass leads to a redistribution of the stress concentrations that glass may be subjected to. The use of glued connections also leads to greater transparency of the structure. Furthermore, one may consider to develop similar charts for other types of structures, for instance facades.

References

- [1] M.Z. Aşık. Laminated Glass Plates: Revealing of Nonlinear Behavior. *Computers and Structures*, **81**, 2659-2671, (2003).
- [2] M.Z. Aşık and S. Tezcan. A Mathematical Model for the Behavior of Laminated Glass Beams. *Computers and Structures*, **83**, 1742-1753, (2005).
- [3] R.A. Behr, J.E. Minor, M.P. Linden, C.V.G. Vallabhan. Laminated Glass Units under Uniform Lateral Pressure. *Journal of Structural Engineering*, **111**, 5, 1037-1050, (1985).
- [4] R.A. Behr, J.E. Minor, M.P. Linden. Load Duration and Interlayer Thickness Effects on Laminated Glass. *Journal of Structural Engineering*. **112**, 6, 1441-1453, (1986).
- [5] R.A. Behr, M.J. Karson, J.E. Minor. Reliability Analysis of Window Glass Failure Pressure Data. *Struct. Safety*, **11**, 43-58, (1991).
- [6] R.A. Behr, J.E. Minor, H.S. Norville. Structural Behavior of Architectural Laminated Glass. *Journal of Structural Engineering*, **119**, 1, 202-222, (1993).
- [7] C. Bength. *Bolt Fixings in Toughened Glass*. Master's thesis, Lund University of Technology, (2005).
- [8] S.J. Bennison, A. Jagota, C.A. Smith. Fracture of Glass/polyvinylbutyral (Butacite) Laminates in Biaxial Flexure. *J. Am. Ceram. Soc.*, **82**, 7, 1761-1770, (1999).
- [9] Boverket. *Regelsamling för konstruktion - Boverkets konstruktionsregler, BKR, byggnadsverkslagen och byggnadsverksförordningen*, Elanders Gotab, Vällingby, (2003).
- [10] R.P.R. Cardoso, J.W. Yoon, M. Mahardika, S. Choudhry, R.J. Alves de Sousa and R.A. Fontes Valente. Enhanced Assumed Strain (EAS) and Assumed Natural Strain (ANS) Methods for One-point Quadrature Solid-shell Elements. *International Journal for Numerical Methods in Engineering*, **75**, 156-187, (2008).
- [11] E. Carrera. Historical Review of Zig-Zag Theories for Multilayered Plates and Shells. *Appl. Mech. Rev.*, **56**, (2003).
- [12] EN 572-1:2004. *Glass in Building - Basic Soda Lime Silicate Glass Products - Part 1: Definitions and General Physical and Mechanical Properties*. CEN, 2004.
- [13] P. Foraboschi. Behavior and Failure Strength of Laminated Glass Beams. *Journal of Engineering Mechanics*, **12**, 1290-1301, (2007).
- [14] C.S. Gerhard. *Finite Element Analysis of Geodesically Stiffened Cylindrical Composite Shells using a Layerwise Theory*, PhD thesis, VPI State Univ., (1994).
- [15] Glafo, Glasforskningsinstitutet. *Boken om glas*. Allkopia, Växjö, (2005).

- [16] M. Haldimann, A. Luible A and M. Overend. *Structural Use of Glass*. Structural Engineering Documents, 10. IABSE, Zürich, (2008).
- [17] G.A. Holzapfel. *Nonlinear Solid Mechanics-A Continuum Approach for Engineering*. John Wiley & Sons Ltd, Chichester, (2010).
- [18] J.A. Hooper. On the Bending of Architectural Laminated Glass. *Int. J. Mech. Sci.*, **15**, 309-323, (1973).
- [19] I.V. Ivanov. Analysis, Modelling, and Optimization of Laminated Glasses as Plane Beam. *International Journal of Solids and Structures*, **43**, 6887-6907, (2006).
- [20] E. Le Bourhis. *Glass-Mechanics and Technology*. Wiley-VHC, Weinheim, (2008).
- [21] J. Malmborg. *A Finite Element Based Design Tool for Point Fixed Laminated Glass*. Master's thesis, Lund University of Technology, (2006).
- [22] J.E. Minor, P.L. Reznik. Failure Strengths of Laminated Glass. *Journal of Structural Engineering*, **116**, 4, 1030-1039, (1990).
- [23] H.S. Norville, K.W. King, J.L. Swofford. Behavior and Strength of Laminated Glass. *Journal of Engineering Mechanics*, **124**, 1, 46-53, (1998).
- [24] J.N. Reddy. *Mechanics of Laminated Composite Plates. Theory and analysis*. CRC Press, Boca Raton, (1997).
- [25] C.V.G. Vallabhan, J.E. Minor, S.R. Nagalla. Stresses in Layered Glass Units and Monolithic Glass Plates. *Journal of Structural Engineering*, **113**, 1, 36-43, (1987).
- [26] C.V.G. Vallabhan, Y.C. Das, M. Magdi, M.Z. Aşık, J.R. Bailey. Analysis of Laminated Glass Units. *Journal of Structural Engineering*, **119**, 5, 1572-1585, (1993).
- [27] A. Van Duser, A. Jagota, S.J. Bennison. Analysis of Glass/polyvinyl Butyral Laminates Subjected to Uniform Pressure. *Journal of Engineering Mechanics*, **125**, 4, 435-442, (1999).

Paper 1

APPLYING SOLID-SHELL ELEMENTS TO LAMINATED GLASS STRUCTURES

MARIA FRÖLING AND KENT PERSSON

Applying Solid-shell Elements to Laminated Glass Structures

Maria Fröling and Kent Persson

Abstract

Solid-shell finite elements are proposed by Maria Fröling and Kent Persson for the efficient and accurate modeling of laminated glass structures. The elements are applied to two test examples and performance is compared to 3D elasticity theory. One example involves a real world structure, where special attention is directed to the prediction of stress distribution around point fixings.

Introduction

Although glass is commonly used as a structural material, knowledge about its mechanical properties and structural behaviour is less than for other structural materials. Therefore, it may be difficult to predict the strength of glass structures, which may result in sudden failures [4]. One alternative to the use of single layered glass is the use of laminated glass, ie two or more layers of glass bonded with plastic interlayers. A major advantage of laminated glass is that a properly designed structure allows for one glass pane to break, while the remaining layers can continue to carry the applied loads.

The combination of very stiff (glass) and very soft (PVB) materials makes a laminated glass pane behave in a complicated manner [1]. The discontinuous stress distributions that may develop in laminated glass panes subject to certain loads and boundary conditions are difficult to model numerically by means of the finite element method. The discontinuities are particularly pronounced around holes and edges and since it is common that the largest stresses occur in these regions, it is important that stress distributions are represented correctly by the model.

The stress distributions are well captured by 3D solid elements but the application of these elements to large real world structures with several point fixings leads to very large models, which are practically impossible to analyse using standard computational resources. One means of overcoming the problem of poor computational efficiency is to use shell elements. However, the shell theories that are required in order accurately to determine stress distributions in laminated glass structures are complicated. In this work, a novel so-called solid-shell finite element [3] is implemented and applied to test examples that comprise laminated glass structures. The element is developed for modeling composite structures with different material properties in each layer.

The reason why the solid-shell element is appropriate for the modeling of this type of composite structures is that the element only requires one element layer per material layer but includes several integration points through thickness. This feature leads to great savings in terms of computational time, still preserving great accuracy.

Implementation of the element is relatively straight-forward. Further advantages compared to shell-elements are that the full 3D constitutive laws are maintained, the use of

rotational degrees of freedom is avoided and that contact situations are more easily modeled through the presence of physical nodes on top and bottom surfaces. The element has proved to be both robust and efficient through extensive testing.

Numerical Tests

In this section, the solid-shell element of [3] is applied to determine the behaviour of laminated glass structures. The accuracy and computational efficiency of the element are evaluated through the analysis of two numerical test problems and comparison is made to 3D elasticity theory (3D solid element).

The first test problem consists of a clamped plate, subjected to a concentrated load. As a second test example, a standard solid-shell element of the commercial finite element software ABAQUS/CAE is applied to a square plate, with a point-fixing in the middle of the plate. This structure has been analysed experimentally and numerically by [2].

The clamped plate is a square plate with a side length of 1000mm. The thickness of one glass layer is 5mm and the thickness of the PVB layer is 0.5mm. Glass and PVB are set to be linear elastic materials. The material parameters for glass are $E = 78$ GPa, $\nu = 0.23$ and $E = 6$ MPa and $\nu = 0.43$ for PVB. A point load is applied on the top glass plate, at the centre of the plate. This load has the size 40000 N. The plate is discretized using 8×8 elements in the x-y plane, and one element per layers in the z-direction.

In figure 1, the deformed structure in 3D is shown. Only top and bottom surfaces of the glass panes are shown. A scale-factor of size $2 \cdot 10^6$ is applied when visualising the results.

The same structure is implemented in ABAQUS/CAE. The element type is a 20 node hexahedral quadratic solid element (C3D20R). The mesh has around 25000 elements. In the model, the symmetry of the structure is utilised and only one quarter of the plate is

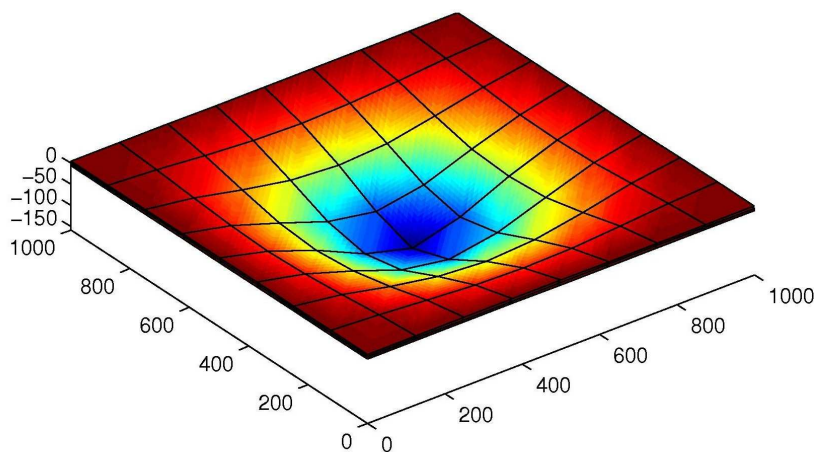


Figure 1: Deformed structure for clamped plate test.

modeled.

Table 1 summarises results for the two models. The variable of interest is the midpoint deflection in the z-direction of the lower glass pane. Also, the numbers of variables of the models are reported. All results are given as fractions of the corresponding result for the 3D model.

For this test, the result using solid-shell elements deviates approximately 10 % from the corresponding result using 3D solids. The model size when the solid-shell elements are used is less than 0.5 % of the model size when 3D solids are used. These results illustrate the relatively good accuracy that is achieved with the use of solid-shell elements but with a very small fraction of the model size for the corresponding model using 3D solids.

In the case of the square plate with point-fixing, the geometry of the structure is that of a 500mm × 500mm plate of laminated toughened glass, with a bolt hole at the centre. The diameter of the hole is 28mm.

For symmetry reasons, only half of the plate is modeled. The model is set up to mimic a compression test, where a compression force is applied on top of a cylindrical bolt affixed to the glass [2]. The glass plate rests on a steel frame with dimensions such that the unsupported area of the glass plate becomes 424mm × 424mm. The bolt has a diameter of 50mm. In the compression test, the top cylindrical metal piece (spreader plate) is put at the location of the bolt hole and a compression force is applied to the bolt.

In the modeling work, some simplifications are made. There is a rubber gasket between the frame and the glass and only this part of the frame is modeled. The same modeling strategy is chosen for the bolt, where an EPDM ring is placed between the bolt and the glass. The inner diameter of the EPDM ring is 34mm.

All materials are modeled as linear elastic. The bolt ring and the rubber gasket are connected to the glass by constraints with the type tie. The rubber gasket is assumed to be locked in all directions. In order to reflect the conditions of the compression test, a deflection of 4.75mm is applied to the top of the EPDM ring. This corresponds to a deflection of the upper glass pane, close to the bolt hole, of approximately 3mm.

The solid-shell element of [3] is not implemented in ABAQUS/CAE. In order to get an idea of the performance of this type of element applied to a structure with a point fixing, a similar element in ABAQUS/CAE is used, namely an eight-node quadrilateral in-plane general-purpose continuum shell element (SC8R) is used for the laminated glass part. For the other parts, standard eight-node linear brick elements (C3D8R) are used. In total, around 11000 elements are used. For comparison, the same model is implemented using 20-node quadratic brick elements (C3D20R). For this model, approximately 32000 elements are used. The finite element meshes for both models are displayed in Figure 2.

Figure 3 shows result graphs for the two models. The result variable is maximum principal

Table 1: Comparison between solid-shell elements and 3D solid elements for clamped plate test.

Element type	Midpoint defl. in z-dir.	No of variables
3D solids (ABAQUS/CAE)	1	1
Solid-shell elements	1.10	0.003

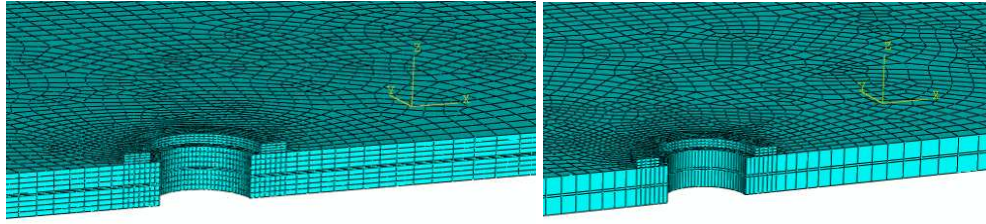


Figure 2: Finite element meshes for the point fixed plate. Left (a) solid element; right (b) solid-shell element.

stress. In the graphs, the location of the maximum values of this variable is concluded to be in the upper glass layer around the bolt fixing, directly above the PVB layer.

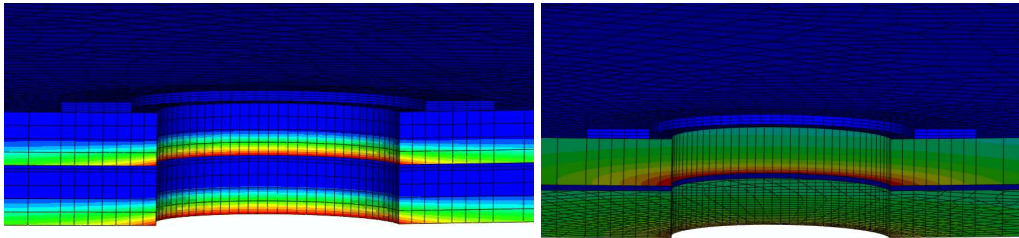


Figure 3: 3D plots of maximum principal stress for the point fixed plate models. Top (a) solid element; Bottom (b) solid-shell element.

Results for maximum principal stress at one corner node close to the hole of the upper glass pane, together with number of variables in the models and CPU times are presented in Table 2. All results are presented as fractions of the corresponding results for the 3D-model.

The experimental mean value of the maximum principal stress at the corresponding location is 1.16 times the corresponding value for the 3D model [2]. The modeling results are in rough accordance with the experimental results. Noteworthy is that when solid-shell elements are used, less than 1% of the CPU time of the corresponding job is required when 3D solid elements are used.

Table 2: Comparison between solid-shell elements and 3D solid elements for point fixed plate test.

Element type	Max princ. stress	No of variables	CPU time
3D solids	1	1	1
Solid-shells	1.04	0.11	0.007

Conclusion and Outlook

In this work, numerical tests have been performed to assess the performance of a relatively new so-called solid-shell element [3]. Overall, performance of the element is good in comparison to standard 3D solid elements but with considerably smaller model sizes and thus, shorter CPU times. For a real-world like glass balustrade with one point-fixing, less than 1% of the CPU time is required when modeling the structure with solid-shells than with 3D solids. Given that the dimensions and number of point-fixings of this structure are small compared to those of real-world structures, it is possible to imagine the great time savings that are obtained when analysing larger and more complex structures using the solid-shell element. The long-term goal of this work is to implement the solid-shell element [3] in a glass design programme, Clear Sight, which has been developed in work by [5]. It is intended that large glass shell structures with an arbitrary number of point fixings could be appropriately designed with standard computer power. The results of the current work show that the solid-shell element is well suited for this purpose.

Acknowledgements

The support from The Swedish Research Council FORMAS, Glasbranschföreningen and Svensk Planglasförening is gratefully acknowledged.

References

- [1] M. Z. Açık and S. Tezcan. A mathematical model for the behavior of laminated glass beams. *Computers and Structures*, 83, 1742-1753, (2005).
- [2] C. Bength. *Bolt fixings in toughened glass*. Master's Thesis, Division of Structural Mechanics at Lund University of Technology, Sweden, (2005).
- [3] R. P. R. Cardoso, J. W. Yoon, M. Mahardika, S. Choudhry, R. J. Alves de Sousa and R. A. Fontes Valente. Enhanced assumed strain (EAS) and assumed natural strain (ANS) methods for one-point quadrature solid-shell elements. *International Journal for Numerical Methods in Engineering*, 75, 156-187, (2008).
- [4] P. Foraboschi. Behavior and failure strength of laminated glass beams. *Journal of Engineering Mechanics*, 133, 12, 1290-1301, (2007).
- [5] J. Malmberg. *A finite element based design tool for point fixed laminated glass*, Master's Thesis, Division of Structural Mechanics at Lund University of Technology, Sweden, (2006).

Paper 2

COMPUTATIONAL METHODS FOR LAMINATED GLASS

MARIA FRÖLING AND KENT PERSSON

Computational Methods for Laminated Glass

Maria Fröling and Kent Persson

Abstract

A new solid-shell finite element is proposed for the purpose of efficient and accurate modeling of laminated glass structures. The element is applied to two test examples and the performance concerning accuracy and efficiency is compared to standard three dimensional solid elements. Further examples illustrate how the element could be applied in the modeling of laminated glass structures with bolted and adhesive joints.

1 Introduction

It is common today to use glass as a structural material. Unfortunately the strength design and structural behavior of glass is less known than for other structural materials like steel, wood or concrete. Thus, there is a risk for inaccurate predictions of the strength of glass structures which could result in sudden failures, [12].

In order to increase safety, laminated glass may be used instead of single layered glass. Laminated glass consists of two or more glass layers bonded with plastic interlayers. The most common material used for the interlayer is polyvinylbutyral, PVB. The use of laminated glass should allow for the glass panes to break while the remaining layers can continue to carry the design loads, and the scattered glass pieces can stick onto the plastic interlayer, and thereby prevent injury.

On the other hand, laminated glass displays a complicated mechanical behavior due to the combination of a very stiff material (glass) and a very soft material (PVB), [4]. A laminated glass-PVB plate is less stiff than a monolithic glass structure of corresponding dimensions, which leads to larger displacements. Furthermore, under certain loads and boundary conditions, discontinuous stress distributions develop in laminated glass structures, ([5], [23]).

Regions close to supports and connections are often subjected to concentrated forces. Since glass is a brittle material that not show plastic deformations before failure, the ability to distribute stresses at load is limited and thus stress concentrations easily develops. Glass fails under tension and in reality the tensile strength is much less than its theoretical counterpart. This is due to the impact of defects on the surface. The defects are created during manufacturing, treatment (such as hole drilling and cutting) and the use of the glass, [5].

The discontinuities of the stress distributions of laminated glass structures are most pronounced around holes and edges, that is, in the regions where the largest stress concentrations often occur, since these regions often are subjected to concentrated forces and may have larger amounts of micro defects. In order to illustrate the discontinuous stress distributions that may arise in a laminated glass structure, a simple example is provided. In Figure 1 below a cantilever beam subjected to bending by a point load at its free end is displayed.

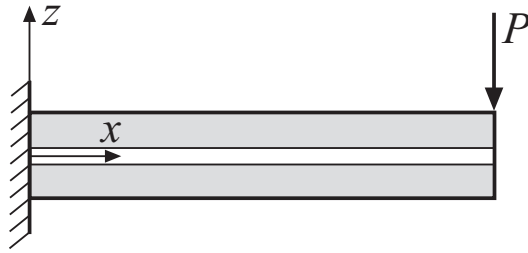


Figure 1: A cantilever laminated glass beam subjected to a point load.

The structure in Figure 1 is modeled by means of the finite element method using two dimensional plane stress elements. The material parameters $E = 78 \text{ GPa}$, $\nu = 0.23$ (glass) and $E = 6 \text{ MPa}$, $\nu = 0.43$ (PVB) are used. The distribution of normal stress along the thickness direction at a cross section located at the center of the beam is shown in Figure 2. As one can see from the figure, the normal stress distributions of the two glass layers are linear as expected. At the glass/PVB interfaces there are discontinuities in the stress distribution and the normal stress in the PVB layer is almost zero. The large difference in stiffness between glass and PVB leads to a shear deformation of the PVB layer and thus to a partial shear force transfer between the glass layers.

It is important for the purpose of safe and cost efficient strength design, that the structural behavior in terms of displacements and stress distributions are accurately determined. Classical design methods, such as simple analytical formulas, do not provide sufficient information in order to determine the stress distributions around bolt connections and determine the load bearing capacity of glass, [14], especially laminated glass. Instead, a finite element model may be used for stress predictions. In order to sufficiently well describe the stress distributions around the bolt connections, a very fine mesh around the bolt holes are required. In comparison to bolted connections, adhesive connections may distribute the load over a greater surface of the glass, leading to a reduction in stress

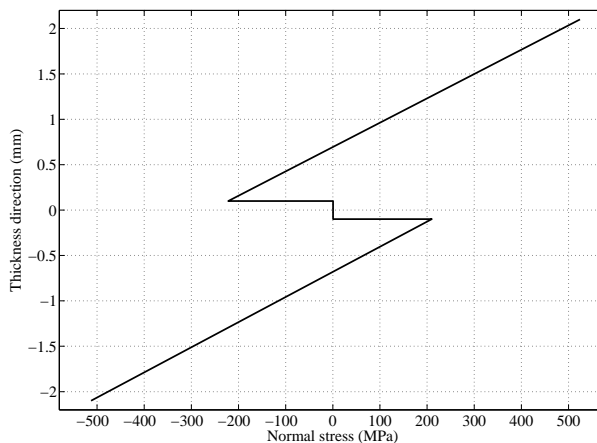


Figure 2: Distribution of normal stress along thickness.

concentrations. Despite this advantage, there are few examples of load bearing adhesive connections used in glass structures and appropriate design guidelines are lacking, [27]. For load bearing adhesive connections, the maximum stresses occur in edge regions of the adhesive layer and for accurate design of the connection it is important to achieve accurate enough stress predictions in these critical regions. Finite element analysis is recommended as a tool for stress prediction, [1].

Accurate predictions of laminated glass strength can be obtained through finite element analyzes using three dimensional solid elements. However, to make precise prediction of the stress distribution several elements must be employed in the thickness direction of each layer resulting in that standard computational resources limit the scope of the analyzes that can be made. Large real world structures with several point fixings are thus practically impossible to analyze, since it easily needs millions of degrees of freedom for a correct result.

According to the classification of [25], a laminated glass plate falls into the category laminated composites, which are made up of layers of different materials. It is possible to reduce the three dimensional elasticity problem to a two dimensional one by making suitable assumptions regarding the kinematics or stress state through the thickness of the laminate. In the simplest of those laminate theories, the kinematic assumptions that straight lines normal to the xy -plane before deformation remain straight after deformation and do not undergo thickness stretching are used. These assumptions are the same as in the classical Kirchhoff and Reissner Mindlin plate theories. The structure is in a state of plane stress. The use of these theories as a basis for a finite element model reduces the model size and increases computational efficiency. However, due to the material discontinuity in the thickness direction of a glass/PVB composite, this structure experiences piecewise continuous displacement and transverse stresses in the thickness direction. The requirements that these two conditions are fulfilled are termed C_z^0 -requirements, [9]. Unfortunately, the two dimensional laminate theories do not fulfill all these demands. The resulting stress distributions are erroneous and the discontinuous stress distribution shown in Figure 2 is not correctly predicted.

An alternative is to use a layerwise laminate theory that contains full three dimensional kinematics and constitutive relations, [25]. The corresponding finite element model possesses some computational advantages compared to a full three dimensional solid element model. These advantages relate to the fact that a two dimensional data structure (two dimensional finite elements) could be used. In the modeling of advanced structures, the layerwise model may however be computationally inefficient, [25], and cumbersome to implement.

Instead it may be appropriate to use so-called solid-shell elements, such as the element presented in [8]. The element is developed for modeling composite structures with different material properties in each layer. In particular, the full three dimensional constitutive laws are maintained allowing for a correct stress distribution prediction, especially at loads and supports. Since the element only requires one element in the thickness direction of each material layer, but includes several integration points through thickness, great computational savings are made and good accuracy is obtained. The implementation of the element is relatively straight-forward. A further advantage compared

to plate or shell element formulations is that contact situations are more easily modeled through the presence of physical nodes on top and bottom surfaces of the element. Of great importance for applications with bolted joints is that the full three dimensional material definition is used and all stress components are calculated which may be important at the supports. The element has proven to be both robust and efficient through extensive testing.

In this work, the solid-shell element in [8] was implemented and applied to test examples comprising laminated glass structures. The accuracy and efficiency of the solid-shell element were examined. The results were compared to the results that were obtained with a three dimensional solid element. Finally, the application of solid-shell elements to real glass structures is illustrated through several examples.

2 The Solid-Shell Concept: An Overview of the Literature

A solid-shell element is a three dimensional solid element which is modified in order to be suited for the analysis of shell-like structures. The modifications are made in a manner so that typical shell properties like bending and in plane stretching can be modeled appropriately using one element in the thickness direction only. When using a low order three dimensional solid element for the modeling of shell-like structures, certain locking phenomena occur. The solid-shells are constructed in a fashion such that locking is prevented.

The solid-shell concept stems from work by [16]. In that paper, several solid-shell elements are presented. Common for these elements is that they all employ the Assumed Natural Strain (ANS) method, [11], to prevent locking. Other contributions to the literature on solid-shell elements are for instance [24] and [17]. [15] discusses several locking phenomena occurring in low order solid-shell elements and the focus is particularly on large deformations' problems. [3] proposes a new class of eight-node solid finite elements. The elements can be used both for three dimensional and thin shell applications. The elements use the Enhanced Assumed Strain (EAS) approach, [26], in order to prevent locking problems. However, the use of the EAS method in these cases leads to poor computational efficiency. The Reduced Enhanced Solid-Shell (RESS) elements presented in ([2], [8]) are eight-node solid-shells. Due to a special one-point quadrature integration scheme, these elements possess considerably higher computational efficiency than their predecessors of [3]. The integration scheme requires only one element layer for a single-layered material, but uses multiple integration points through thickness. This leads to high computational efficiency and great accuracy. The reduced integration scheme requires physical stabilization to prevent zero-energy modes. The stabilization method of [7] and the ANS method are employed for this purpose. In order for the Modified RESS (M-RESS) element, [8], to pass the membrane patch test, the stabilization method based on results of ([22], [21]) is used. For instance the B-bar approach, [18], is used in order to alleviate locking problems that occur due to the stabilization procedure. The EAS method, [26], plays an important role in preventing various types of other locking problems that

occur in the element formulation.

The M-RESS element is particularly suited to use for the application to laminated glass, since the reduced integration scheme allows that only one element layer is used per material layer, which greatly reduces the computational efficiency. The excellent performance of the element, and the fact that implementation guidelines are straightforward further motivates the choice of this element for use for computations of glass structures.

3 Brief Description of the M-RESS Element

3.1 M-RESS and the EAS-method

M-RESS stands for Modified Reduced (in-plane) integration, Enhanced strain field, Solid-Shell element. The geometry of the element is that of a three dimensional hexahedral solid element with eight nodes and three translational degrees of freedom per node. The geometry of the element, together with the coordinate systems involved, is shown in Figure 3.

The M-RESS element is based on the Enhanced Assumed Strain (EAS) approach, [26]. The EAS method plays an important role in reducing volumetric and Poisson locking. The crucial point of the EAS method is to enlarge the strain field, ε , through adding a new field of enhanced strain parameters, α . It can be shown (see for instance [2]) that only one enhancing parameter, α_1 , is enough in order to reduce the locking problems. This means that the locking problems can be reduced considerably, while maintaining high computational efficiency of the element formulation which is achieved through the reduced integration of having multiple integration points along the local ζ -axis only. To overcome the hourglass modes that then may develop, hourglass stabilization is made by the Assumed Natural Strain (ANS) method for the transverse shear components whereas the membrane field were stabilized based on the stabilization vectors of [22].

In the local frame, the enhanced strain field is added to the ordinary strain field:

$$\tilde{\varepsilon} = \varepsilon + \varepsilon_\alpha = [\hat{\mathbf{B}}_u \hat{\mathbf{B}}_\alpha] \begin{bmatrix} \mathbf{u} \\ \alpha \end{bmatrix} = \tilde{\mathbf{B}}\tilde{\mathbf{u}}. \quad (1)$$

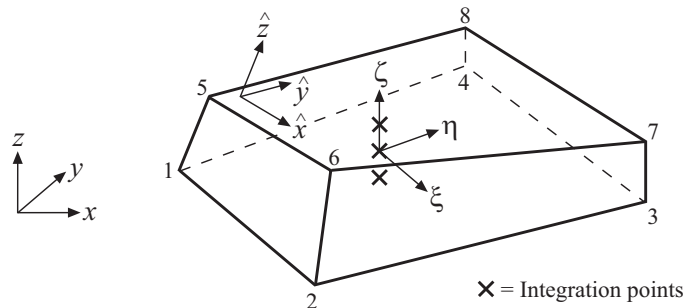


Figure 3: Element geometry.

$\hat{\mathbf{B}}_{\mathbf{u}}$ is the standard FEM strain-displacement matrix. $\boldsymbol{\varepsilon}_{\alpha}$ is the enhanced part of the strain field. In the convective coordinate system, the enhanced strain field is chosen as:

$$\boldsymbol{\varepsilon}_{\zeta\zeta}^{\alpha} = \zeta\alpha_1, \quad (2)$$

which leads to the following enhanced strain-displacement matrix in the local coordinate system:

$$\hat{\mathbf{B}}_{\alpha} = \mathbf{Q}_0[000\zeta00]^T. \quad (3)$$

For a definition of the transformation matrix \mathbf{Q}_0 , see [8] and references therein. For linear applications, the application of the EAS method leads to the following system of equations, [26]:

$$\begin{bmatrix} \hat{\mathbf{K}}^{\mathbf{u}\mathbf{u}} & \hat{\mathbf{K}}^{\mathbf{u}\alpha} \\ \hat{\mathbf{K}}^{\alpha\mathbf{u}} & \hat{\mathbf{K}}^{\alpha\alpha} \end{bmatrix} \begin{pmatrix} \mathbf{u} \\ \alpha \end{pmatrix} = \begin{pmatrix} \mathbf{f}^{ext} \\ \mathbf{0} \end{pmatrix}. \quad (4)$$

Static condensation of α can be performed on (4) that leads to:

$$\hat{\mathbf{K}}^{\mathbf{u}+\alpha} = \hat{\mathbf{K}}^{\mathbf{u}\mathbf{u}} - \hat{\mathbf{K}}^{\mathbf{u}\alpha}(\hat{\mathbf{K}}^{\alpha\alpha})^{-1}\hat{\mathbf{K}}^{\alpha\mathbf{u}}. \quad (5)$$

The physical stabilization procedure adds an extra part, $\hat{\mathbf{K}}^H$, to the stiffness matrix as follows:

$$\hat{\mathbf{K}} = \hat{\mathbf{K}}^{\mathbf{u}+\alpha} + \hat{\mathbf{K}}^H. \quad (6)$$

The displacement field can now be obtained as:

$$\mathbf{u} = (\hat{\mathbf{K}})^{-1}\mathbf{f}^{ext}. \quad (7)$$

3.2 Strain Field

For the application of the physical stabilization method, a division of the strain tensor into membrane, normal and transverse shear components is necessary. In the convective coordinate system the strain tensor can be written as:

$$\boldsymbol{\varepsilon} = [\boldsymbol{\varepsilon}_m \dots \boldsymbol{\varepsilon}_n \dots \boldsymbol{\varepsilon}_s]^T = [\boldsymbol{\varepsilon}_{\xi\xi} \boldsymbol{\varepsilon}_{\eta\eta} \boldsymbol{\varepsilon}_{\zeta\zeta} \dots \boldsymbol{\varepsilon}_{\zeta\xi} \dots \boldsymbol{\varepsilon}_{\xi\zeta} \boldsymbol{\varepsilon}_{\eta\zeta}]^T, \quad (8)$$

where the strain components are defined as:

$$\boldsymbol{\varepsilon}_{ab} = \frac{1}{2}(\mathbf{J}_{,a}\mathbf{u}_{,b} + \mathbf{J}_{,b}\mathbf{u}_{,a}), \quad (a, b = \xi, \eta, \zeta), \quad (9)$$

where $\mathbf{J}_{,a}$ are the lines of the Jacobian matrix \mathbf{J} .

The strain tensor in the local coordinate system is given by

$$\hat{\boldsymbol{\varepsilon}} = \mathbf{Q}_0\boldsymbol{\varepsilon}, \quad (10)$$

where \mathbf{Q}_0 is defined as in [8] and references therein.

It can be shown, see [8], that the total strain field can be expanded to constant, linear and bilinear terms in the coordinates ξ , η and ζ . The constant membrane strain field is composed of a component evaluated at the center of the element and a component that depends only on the ζ coordinate:

$$\boldsymbol{\varepsilon}_{ml}^C = \boldsymbol{\varepsilon}_m^0 + \zeta \boldsymbol{\varepsilon}_m^\zeta. \quad (11)$$

The constant membrane strain tensor must be transformed to the local coordinate system through the transformation (10). For a detailed description of the corresponding strain-displacement matrices, see [8].

The reduced integration scheme with integration points only along the ζ -axis will lead to the cancellation of the contributions to the strain-displacement matrix that are corresponding to the non-constant terms of the strain field. Physical stabilization strain-displacement relations are therefore required for those terms. The membrane part of the stabilization strain tensor is given by:

$$\boldsymbol{\varepsilon}_{ml}^H = \xi \boldsymbol{\varepsilon}_m^\xi + \eta \boldsymbol{\varepsilon}_m^\eta + \xi \eta \boldsymbol{\varepsilon}_m^{\xi\eta} + \xi \zeta \boldsymbol{\varepsilon}_m^{\xi\zeta} + \eta \zeta \boldsymbol{\varepsilon}_m^{\eta\zeta}. \quad (12)$$

The strain tensor is transformed to the local coordinate system through the application of (10). Explicit descriptions of the corresponding strain-displacement matrices are given in [8].

The ANS-method is used in order to construct strain-displacement stabilization matrices for the normal strain component $\boldsymbol{\varepsilon}_{\xi\xi}$ and for the transverse shear strains $\boldsymbol{\varepsilon}_{\xi\zeta}$ and $\boldsymbol{\varepsilon}_{\eta\zeta}$. For a description of the application of the ANS-method, we refer to [8].

A second stabilization method is applied to the membrane strain components in order to make the M-RESS element pass the membrane patch test. Bases for the method are provided in ([22], [21]).

To eliminate volumetric locking that occurs due to the stabilization procedure, the B-bar method, [18], is used. When applying the B-bar method in the local coordinate system, the strain-displacement operator corresponding to the physical stabilization scheme is divided into its dilatational and deviatoric components, and only the deviatoric part is used for stabilization. See [8] for details. The resulting strain-displacement matrices for the hourglass membrane field are given in [8].

It should be noted that the stabilization scheme requires that the nodal degrees of freedom are specified in the local coordinate system. The following transformation from global coordinates to local coordinates is therefore used:

$$\hat{\mathbf{d}}_I = \hat{\mathbf{R}}_0 \cdot \mathbf{d}_I. \quad (13)$$

$\hat{\mathbf{R}}_0$ is defined in [8].

The resulting membrane strain tensor for the hourglass field is defined as

$$\hat{\boldsymbol{\varepsilon}}_m^H = \begin{bmatrix} \hat{\boldsymbol{\varepsilon}}_{\hat{x}\hat{x}} \\ \hat{\boldsymbol{\varepsilon}}_{\hat{y}\hat{y}} \\ \hat{\boldsymbol{\varepsilon}}_{\hat{x}\hat{y}} \end{bmatrix} = (\xi \cdot \hat{\mathbf{B}}_{ml}^\xi + \eta \cdot \hat{\mathbf{B}}_{ml}^\eta + \xi \eta \cdot \hat{\mathbf{B}}_{ml}^{\xi\eta} + \xi \zeta \cdot \hat{\mathbf{B}}_{ml}^{\xi\zeta} + \eta \zeta \cdot \hat{\mathbf{B}}_{ml}^{\eta\zeta}) \cdot \hat{\mathbf{R}}_0 \cdot \mathbf{d}_I. \quad (14)$$

3.3 Stress Evaluation

The displacements obtained from (7) are used together with equation (1) in order to compute the strain field, $\tilde{\epsilon}$. Once the strain distribution has been determined, the stress distribution is given by:

$$\sigma = \mathbf{D}\tilde{\epsilon} = \mathbf{D} \cdot [\hat{\mathbf{B}}_u \hat{\mathbf{B}}_\alpha] \begin{bmatrix} \mathbf{u} \\ \alpha \end{bmatrix}. \quad (15)$$

\mathbf{D} is the constitutive matrix. The stresses are evaluated at the integration points. A stress smoothing procedure based on a quadratic least squares fit is used in order to extrapolate and average the stresses at the nodes, [10].

4 Numerical Examples

The M-RESS element described in the previous section was applied to a simple test example comprising laminated glass and a convergence analysis. The accuracy and computational efficiency of the element were evaluated through the analysis of the test problems and comparison was made to three dimensional solid elements. In the first test example, a cantilever beam made of laminated glass was loaded with a point load in the negative z -direction. The convergence analysis comprised a clamped laminated glass plate with a distributed load applied at the top surface.

4.1 Cantilever Beam

First, the M-RESS element was implemented and tested using a simple test problem comprising a cantilever beam of laminated glass subjected to a point load at the tip of the beam. The x - y dimensions of the beam were 100×10 . The laminate consisted of two glass layers with a PVB interlayer. An illustration of the beam in the xz -plane is provided in Figure 4. Glass and PVB were set to be linear elastic materials. The material parameters were the modulus of elasticity, E and Poisson's ratio, ν . For glass $E = 78$ GPa and $\nu = 0.23$ and for PVB $E = 6$ MPa and $\nu = 0.43$. The point load $F = 4000$ N and was directed in the negative z -direction.

The example was modeled using Matlab. Two different values of the thickness, t , were employed, namely $t = 2.1$ and $t = 4.2$. For the first case, the thickness of the glass layers,

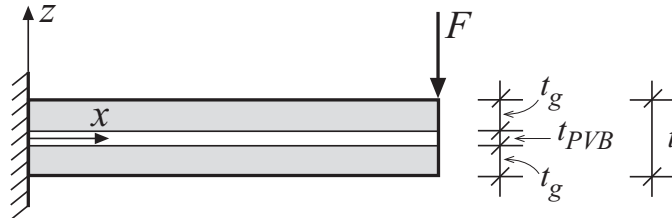


Figure 4: Two dimensional geometry of cantilever beam.

$t_g = 1$ and the thickness of the PVB layer, $t_{PVB} = 0.1$. For the second case, $t_g = 2$ and $t_{PVB} = 0.2$.

The beam was discretized using four different discretizations in the xy-plane, and one element per material layer in the z-direction.

The test problem was also modeled using ABAQUS. The element type was a 20-node quadratic brick element (C3D20R). The mesh was discretized using four different discretizations in the xy-plane and four elements per material layer in the z-direction.

Results from the analysis with a total thickness $t = 2.1$ are presented in Table 1 for the M-RESS element. The presented quantities are the vertical deflection at the tip of the beam, the maximum normal stress component in the x-direction and the number of variables in the model. The maximum normal stress component is given for a cross section at the middle of the beam in the x-direction. The first two measured quantities are structural mechanical quantities and reflect the accuracy of the element. The last quantity is related to the computational efficiency of the element. All structural mechanical quantities are represented as fractions of the results achieved when the finest mesh is used. The number of variables are taken as fractions of the number of variables for the finest mesh when a three dimensional solid element is used, see below.

Similar results for the three dimensional solid element are presented in Table 2.

The corresponding results for $t = 4.2$ are reported in Tables 3 and 4.

For the thickness, t , equal to 2.1, both the M-RESS element and the solid element show good convergence. The results for both the vertical tip displacement, w_{tip} , and the normal stress in the x-direction, σ_{xx} , have converged within reasonable limits ($+/- 5\%$ from the corresponding results for the finest discretized model respectively) using the 20×2 discretization in the xy-plane. The M-RESS element model uses only around 0.7 % of the variables of the finest discretized solid element model, compared to around 8 % for the solid element model of the same discretization. When t is equal to 4.2, only 0.2 % of the finest model size for the solid element is required for the M-RESS element to yield convergence.

Table 1: Results for cantilever beam test for M-RESS element, $t = 2.1$.

Mesh	w_{tip}	σ_{xx}	Number of variables
$10 \times 1 \times 1$	0.997	0.934	0.0024
$20 \times 2 \times 1$	0.999	1.020	0.0070
$40 \times 4 \times 1$	1.000	1.000	0.0228
$80 \times 8 \times 1$	1.000	1.000	0.0810

Table 2: Results for cantilever beam test for solid element, $t = 2.1$.

Mesh	w_{tip}	σ_{xx}	Number of variables
$10 \times 1 \times 4$	1.317	1.002	0.0265
$20 \times 2 \times 4$	1.000	0.999	0.0806
$40 \times 4 \times 4$	1.000	1.000	0.2737
$80 \times 8 \times 4$	1.000	1.000	1.000

Table 3: Results for cantilever beam test for M-RESS element, $t = 4.2$.

Mesh	w_{tip}	σ_{xx}	Number of variables
$10 \times 1 \times 1$	0.998	0.974	0.0024
$20 \times 2 \times 1$	0.999	1.003	0.0070
$40 \times 4 \times 1$	1.000	1.000	0.0228
$80 \times 8 \times 1$	1.000	1.000	0.0810

Table 4: Results for cantilever beam test for solid element, $t = 4.2$.

Mesh	w_{tip}	σ_{xx}	Number of variables
$10 \times 1 \times 4$	1.326	1.000	0.0265
$20 \times 2 \times 4$	1.000	1.000	0.0806
$40 \times 4 \times 4$	1.000	1.000	0.2737
$80 \times 8 \times 4$	1.000	1.000	1.000

This test example points to that the M-RESS element is more efficient than a second order three dimensional solid element when it comes to modeling laminated glass. However, the results above are not optimized when it comes to mesh size and one should be careful to draw any conclusion regarding relative efficiency of the two elements. In the next section, a more rigorous convergence study is made which shows the relative performance of the elements in a more clear way.

The ability of the M-RESS element to represent the discontinuous stress distribution that arises in the thickness direction of laminated glass is demonstrated in Figure 5. The stress distribution for σ_{xx} is shown for a cross section at $x = 50$. The results from simulations using the finest discretized mesh for the M-RESS element is taken as reference solution and the stress distribution for the $10 \times 1 \times 1$ mesh is chosen to illustrate the efficiency of the M-RESS element.

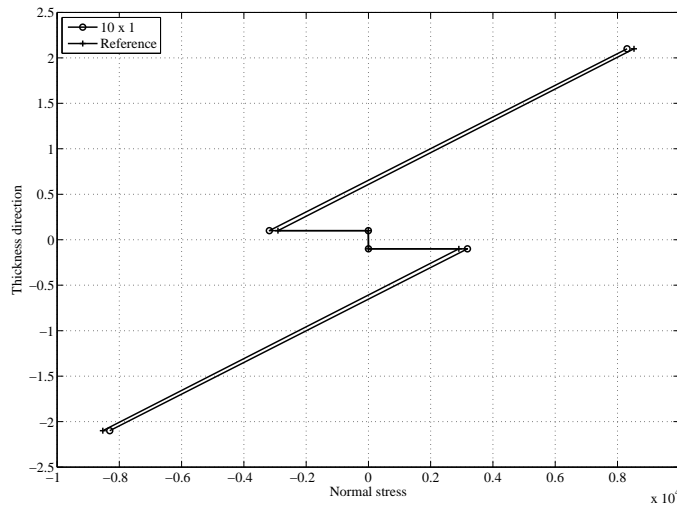


Figure 5: Distribution of normal stress along thickness, cantilever beam test, $t = 4.2$.

From the figure it is clear that the use of the M-RESS element produces results that are representing the σ_{xx} distribution in the z-direction well, for a relatively coarse mesh.

4.2 Convergence Analysis

This convergency analysis comprised of a clamped square plate of a laminated glass loaded by a pressure surface load, Figure 6. The laminate consisted of two glass panes and one intermediate layer made of PVB. The surface load of 4000 per unit area acted on the surface of the uppermost glass pane. The in-plane dimensions of the plate were 1000×1000 and the total thickness was 21 whereas the glass thickness was 10 and the interlayer thickness 1. Both glass and PVB were modeled as linear elastic materials and the same material parameters as for the cantilever beam test were used. The plate was clamped, thus all displacements of the four sides were constrained to zero.

Three different elements were tested in the finite element analysis of the plate; the M-RESS element, a linear 8-node (C3D8R) and a quadratic 20-node element (C3D20R), both standard isoparametric quadrilateral elements with reduced integration. The analyses with the 8- and 20-node elements were made using the commercial FE package ABAQUS and the analyses with the M-RESS element were made using Matlab. For the M-RESS element, one element for each material layer was used in the thickness direction whereas the 8-node element required four elements and the 20-node two elements for each element layer to reach a reasonable convergence rate.

To evaluate the models, the in-plane stress in one direction and the vertical displacement at the center point of the bottom glass surface were compared. Results from the convergence analysis are shown in Figures 7 and 8. The results in the figures were normalized to the results using the 20-node element and 2 millions degrees of freedom.

The 8-node element showed very poor convergence rate for the clamped laminated plate structure. Not even by using 500.000 degrees of freedom the element reached a sufficient result, especially not for the stresses that showed about 20 % error. The 20-node element showed much better convergence rate as shown in Figure 8. About 3000 degrees of freedom was needed to get less than 5 % error for both the displacements and the stresses. The M-RESS element that performed extremely well and only required about 300 degrees of

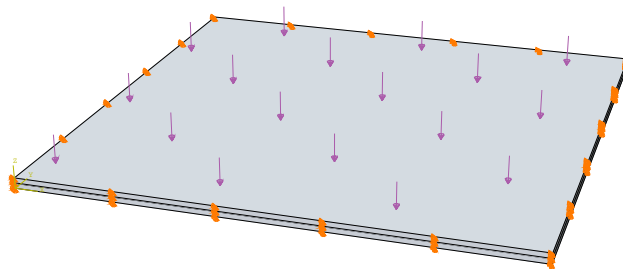


Figure 6: Geometry of the clamped plate.

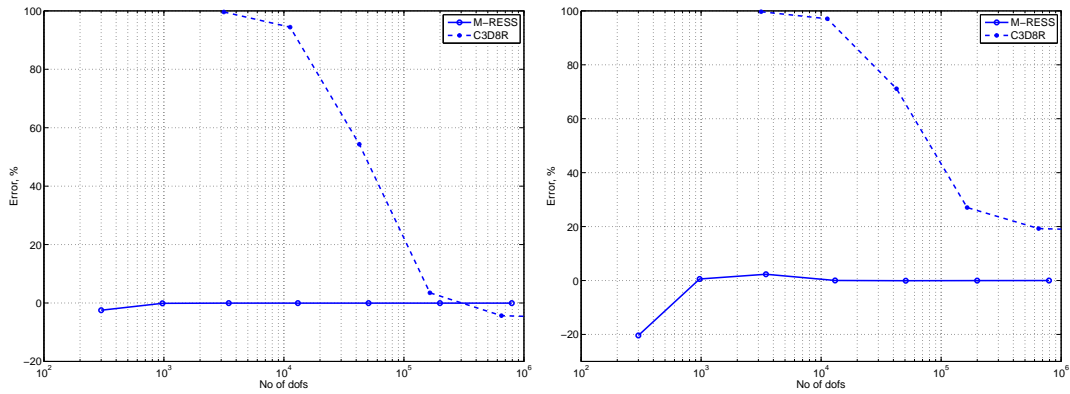


Figure 7: Comparison of the M-RESS and the 8-node quadrilateral element, displacement versus number of degrees of freedom to the left and stress versus number of degrees of freedom to the right.

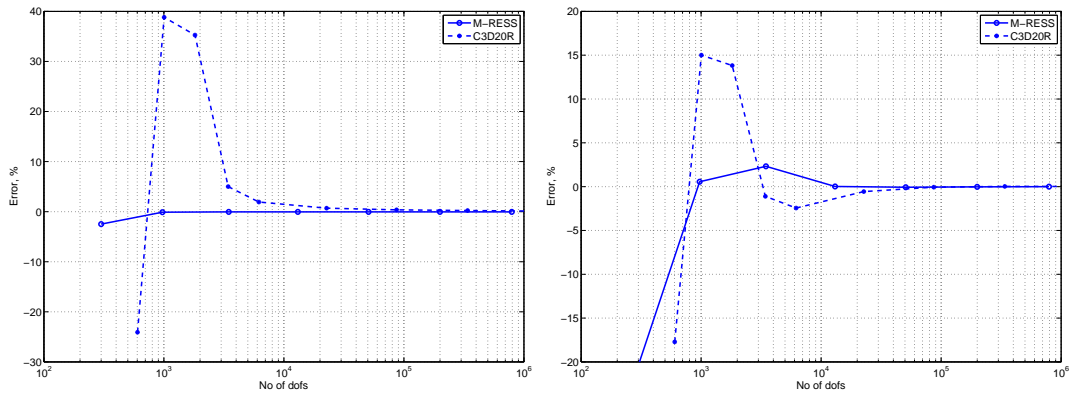


Figure 8: Comparison of the M-RESS and the 20-node quadrilateral element, displacement versus number of degrees of freedom to the left and stress versus number of degrees of freedom to the right.

freedom to get less than 5 % error for the displacements and about 700 degrees of freedom for the stresses to get less than 5 % error.

A conclusion is that standard isoparametric elements with linear approximating functions is not recommended for analyzing laminated glass and the M-RESS element is an excellent choice for analyzing laminated glass.

5 Application to Glass Structures

In the previous section the ability of the M-RESS element to represent displacements and stress distributions of laminated glass structures is demonstrated. In order to fully illustrate the usefulness of the approach, this section deals with the application of the M-RESS element to several real glass structures comprising laminated glass. All examples

comprise supports and joints. The glass supports are either bolted or adhesive. In the regions where the stress concentrations are expected, local mesh refinement is required. When analysing real glass structures of large dimensions that contains several bolt or adhesive connections, the total finite element model will be large and the scope of the solid-shell concept is particularly useful in order to decrease the model size and to reduce the computational requirements of memory and time.

5.1 Laminated Glass with Bolt Connection

In the following example, a finite element model was made of an experimental test where a square glass plate with one bolt connection is subjected to a compressive force. The aim of the experimental test was to determine the strength of glass around a bolt fixing. The commercial finite element programme ABAQUS was used for the simulations.

The geometry of the glass specimen is shown in Figure 9.

In the experimental set-up, the glass plate rested on a steel frame of size $500 \times 500 \times 38$ mm. Thus, the unsupported area of the glass specimen was 424×424 mm. A rubber gasket was placed between the glass and the steel. A cylindrical bolt was placed on the top of the glass, at the middle of the plate, and a compressive force was applied to the bolt. The bolt had an outer diameter of 50 mm and the hole was 28 mm in diameter.

Strain gauges were glued on the glass on the tension side at the hole edge. A test series was performed and the ultimate tensile stress, σ_{max} , for each test, the mean ultimate tensile stress, σ_{mean} , for the whole test series and the maximum compressive force, F_{max} , for each test are calculated, [5]. The results are reported in Table 5.

Since the steel frame was regarded as rigid, only the rubber gasket between the steel frame

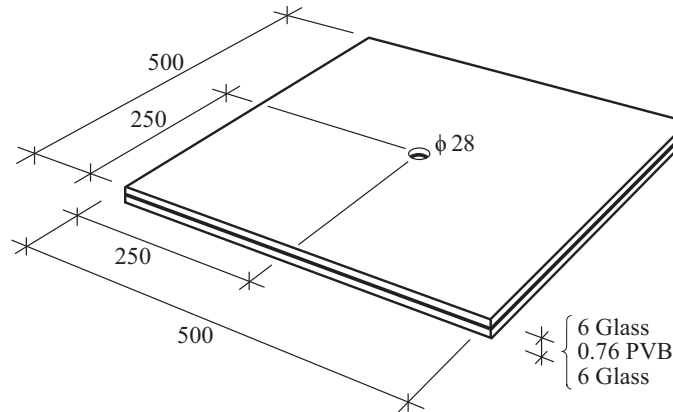


Figure 9: Geometry of glass plate.

Table 5: Test results.

	Test 1	Test 2	Test 3	Test 4	Test 5	Test 6	Mean
σ_{max} (MPa)	174.91	201.88	180.78	173.29	154.38	177.52	177.13
F_{max} (kN)	4.81	4.70	4.75	4.56	4.25	4.57	4.61

and the glass plate was modeled. Similarly, the bolt has an EPDM ring that protects the glass from direct contact with the steel bolt. Only the EPDM ring was modeled. The inner diameter of the EPDM ring was 34 mm and the ring had a thickness of 3 mm.

Due to symmetry, only half of the plate was modeled.

All materials were modeled as linear elastic and isotropic and the material parameters are shown in Table 6.

Since no slip between the rubber and the glass was expected, a full tie constraint was applied. The load for the compression test was set to the mean value of the maximum force from the experimental tests, see Table 5. The load was applied on the top of the EPDM ring. Along the symmetry line, symmetry boundary conditions were applied. The rubber frame was constrained to zero displacement in all directions.

The M-RESS element was used in the modeling of the laminated glass plate. For the other parts of the model, a standard eight-node linear brick element (C3D8R) was employed. The model contained around 11000 elements. The laminated glass part had one element layer per material layer and the EPDM ring as well as the rubber gasket parts had three element layers in the thickness direction. In Figure 10, the finite element mesh for the whole structure in the vicinity of the bolt hole is displayed. As can be seen, the mesh was refined close to the bolt hole.

As a comparison, numerical tests were performed by use of ABAQUS and 20-node second

Table 6: Material parameters for model.

Material	E (MPa)	ν
Glass	78000	0.23
PVB	5.2	0.45
Rubber	1	0.45
EPDM	7	0

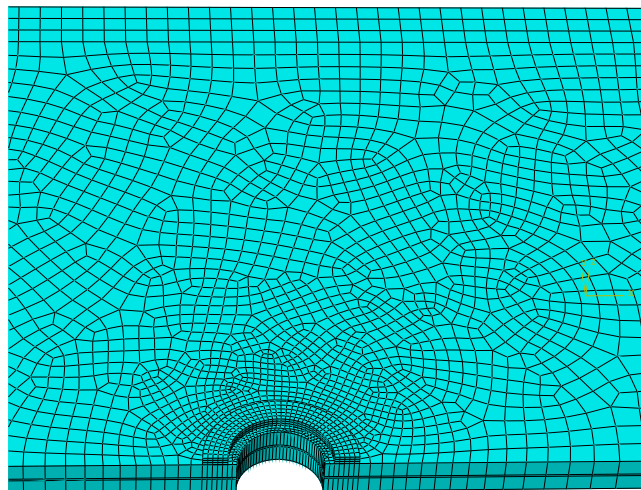


Figure 10: Finite element mesh for square plate model.

order solid elements (C3D20R). When solid elements were used, four element layers per glass layer and two element layers for the PVB layer were employed. The whole model contained approximately 34000 elements.

In finite element analyses of the laminated glass plate, the results show that the largest maximum principal stresses are located in the upper glass layer, close to the bolt fixing, as expected. The distribution of the maximum principal stresses in the glass plate close to the bolt fixing is shown in Figure 11.

As a quantitative comparison, the maximum principal stress at an element close to the hole edge in the lower glass layer was determined for the models applying M-RESS elements and C3D20R respectively. These correspond to the values of the maximum principal stress determined experimentally. The results are presented in Table 7. Observe that the experimental values of the maximum principal stress are not the maximum values that arise in the structure. There was no possibility to glue the strain gauges in between the glass layers, where the maximum principal stresses do occur.

The model size of the finite element model with M-RESS elements was only 10 % of that of the model with solid elements.

The result by applying the M-RESS element is very good for modeling a laminated glass structure with bolts. The element predicts stresses as accurate as the second order solid element with only 10 % of the model size of that element. The correspondance between simulations and experiments is fair and the modeling results are accurate enough to be used in practical design of glass structures. The discrepancy between the experimental and simulation results are probably due to that the properties of the PVB-layer not were accurate enough.

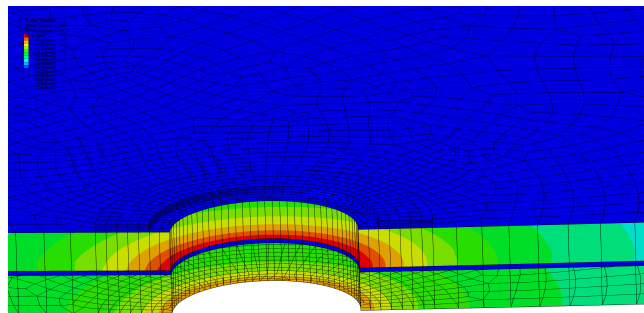


Figure 11: Maximum principal stress close to bolt connection.

Table 7: Maximum principal stress close to bore hole.

	Maximum principal stress (MPa)
Experimental mean value	177.1
M-RESS	159.2
C3D20R	153.4

5.2 Glass Beam with Adhesive Joint

This example deals with the finite element modeling of an experimental test with the aim of determining the shear capacity of an adhesive joint in a large dimension glass beam.

A series of tests consisting of a four-point bending test of a beam with a three meter span were conducted. The beams were constructed by three flat-glass elements measuring $250 \times 2000 \text{ mm}^2$ with a width of 12 mm. They were joined in overlap joints at the middle of the three meter span by two adhesive joints each measuring $250 \times 250 \text{ mm}$. The arrangement of three glass elements was chosen to create a symmetrical beam in order to obtain pure shear stresses in the joints, see Figure 12.

Five types of adhesives were tested consisting of three stiff adhesives; a UV curing acrylate, a polyurethane glue and an epoxy, and two soft, rubber-like, adhesives based on silyl modified polymers (SMP), commonly found as adhesives in automotive glass gluing. The adhesive layers were about 0.2 mm in thickness for the stiff adhesives and about 2 mm for the soft adhesives. The tests revealed that a soft weak SMP-based adhesive may, for a large shear-joint, result in a stronger joint than for using a stiff strong adhesive, see Table 8.

Tests were also conducted on small specimens ($20 \times 20 \text{ mm}^2$) to evaluate material properties and material models for the various types of adhesives, [20]. These material properties

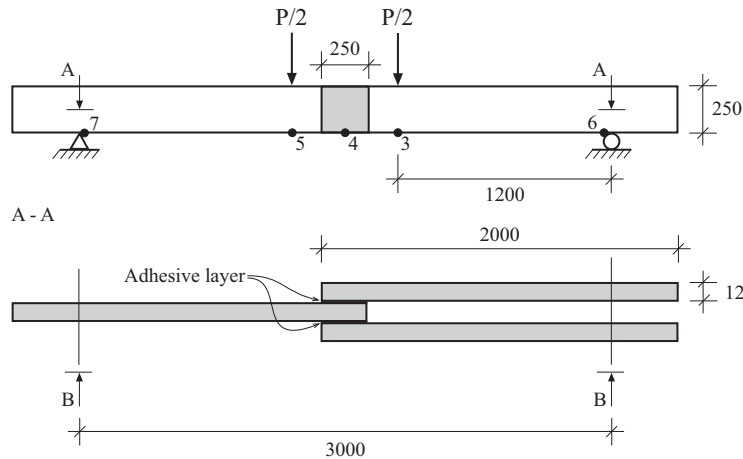


Figure 12: Test setup of four-point bending test of glass beam with adhesive joint.

Table 8: Ultimate load and deformations at the mid-point of the beam.

Type of adhesive	Total applied load (kN)	Displacement (mm)
SMP type 1	49.3	51
SMP type 2	48.8	50
Epoxy	30.3	10
Polyurethane	10.3	3.5
UV-curing glue	22.3	7.5

were utilized in the finite element modeling of the jointed beam.

In order to evaluate the tested adhesives the glass beam was simulated in ABAQUS both by use of the M-RESS element and an eight node three-dimensional quadratic solid element (C3D20R). Here, the results from the simulation with the epoxy adhesive are presented and a comparison is made from using the two element types. The flat glass elements were modeled as three dimensional objects with a Young's Modulus of 70 GPa and a Poisson's ratio of 0.23. The epoxy joint was modelled according to the evaluated material model from the tests of the small specimens to a Young's Modulus of 1500 MPa and a Poisson's ratio of 0.25.

To ensure that the load was applied symmetrical, the load was applied on a reference point coupled to nodes by a kinematic coupling constraint. The load was applied as a displacement of the reference point. The magnitude of the displacement was -0.006 m in the load direction. All other possible displacements of the reference point were constrained to zero. At the supports, displacements were prevented in the load direction and in the thickness direction of the beam.

In the finite element model with M-RESS elements, one element layer per material layer was applied in the thickness direction. The model contained approximately 16000 elements. For three-dimensional solid elements, the model contained about 34000 elements. As a comparison between experimental results and the results from the finite element simulations, the displacement in the load direction at point 4 of Figure 12 was taken as test variable. Results from experiment and simulations are presented in Table 9. Both of the finite element models give accurate enough results, and it is noted that the model with M-RESS elements requires merely 20 % of the model size of the model with solid elements.

For the stiffer adhesives, stress-concentrations occurred at the corners of the joint and consequently the critical shear stress was first reached there. For the silicones the stresses were more evenly distributed, the concentrations were observed at the edges of the joint and of less magnitude than in the stiffer adhesives. The principal pattern of the stress distribution is shown in Figure 13.

From the results it is shown that the concentration of stresses plays a decisive role in the ultimate load of the joints. The apparently stronger glues turn out to have less ultimate load than the silicones due to the high magnitude of the stress-concentrations in the corners. The only glue to compete with the silicones is the Epoxy, which due to its high ultimate shear stress supports the stress concentrations better.

Table 9: Ultimate deformations at the mid-point of the beam.

Test	Displacement (mm)
Experimental	10.00
M-RESS	10.20
C3D20R	10.24

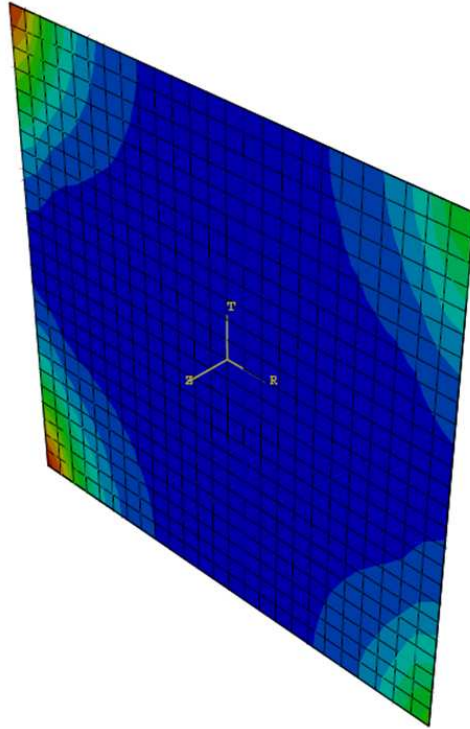


Figure 13: Shear stress distribution for adhesive layer.

6 Conclusions

This paper deals with accurate and efficient methods to perform finite element analyses of laminated glass structures. The solid-shell element of [8] is suggested as an excellent choice to use for the finite element simulations. The element was tested using two test examples comprising thin structures of laminated glass subjected to bending. Comparison is made to three dimensional solid elements. It is demonstrated that the M-RESS element produces accurate results for displacements and stresses with a relatively small fraction of the model size of the corresponding solid element model. The computational time is increasing between square and cubic with the model size, which means that the use of the M-RESS element instead of three dimensional solid elements decreases computational time significantly.

The M-RESS element was further evaluated by analyzing two glass structures with bolted and adhesive joints respectively and comparing with experimental results. The finite element software ABAQUS was used for the examples. The tests illustrate the solid-shell element applied to laminated glass structures where joints are used and show a successful prediction of displacements and stresses with a considerable increase in computational efficiency. The real advantage of the solid-shell concept is for the use in the analyses of structures that are even more complicated than the examples shown. For these cases, the use of the M-RESS element might make it possible to perform finite element analyses us-

ing standard computational resources, whereas the models would become too large using conventional three dimensional solid elements.

References

- [1] R.D. Adams and J.A. Harris. The Influence of Local Geometry on the Strength of Adhesive Joints. *International Journal of Adhesion and Adhesives*, **7**, 2, 69-80, (1987).
- [2] R.J. Alves de Sousa, R.P.R. Cardoso, R.A. Fontes Valente, J.W. Yoon, J.J. Grácio and R.M. Natal Jorge. A New One-point Quadrature Enhanced Assumed Strain (EAS) Solid-shell Element with Multiple Integration Points Along Thickness: Part 1 - Geometrically Linear Applications. *International Journal for Numerical Methods in Engineering*, **62**, 952-977, (2005).
- [3] R.J. Alves de Sousa, R.M. Natal Jorge, R.A. Fontes Valente and J.M.A. César de Sá. A New Volumetric and Shear Locking-free 3D Enhanced Strain Element. *Engineering Computations*, **20**, 896-925, (2003).
- [4] M.Z. Açı̇k and S. Tezcan. A Mathematical Model for the Behavior of Laminated Glass Beams. *Computers and Structures*, **83**, 1742-1753, (2005).
- [5] C. Bength. *Bolt Fixings in Toughened Glass*. Master's thesis, Lund University of Technology, (2005).
- [6] Boverket. *Regelsamling för konstruktion - Boverkets konstruktionsregler, BKR, byggnadsverkslagen och byggnadsverksförordningen*. Elanders Gotab, Vällingby, (2003).
- [7] R.P.R. Cardoso, J.W. Yoon, J.J. Grácio, F. Barlat, J.M.A. César de Sá. Development of a One Point Quadrature Shell Element for Nonlinear Application with Contact and Anisotropy. *Computer Methods in Applied Mechanics and Engineering*, **191**, 5177-5206, (2002).
- [8] R.P.R. Cardoso, J.W. Yoon, M. Mahardika, S. Choudhry, R.J. Alves de Sousa and R.A. Fontes Valente. Enhanced Assumed Strain (EAS) and Assumed Natural Strain (ANS) Methods for One-point Quadrature Solid-shell Elements. *International Journal for Numerical Methods in Engineering*, **75**, 156-187, (2008).
- [9] E. Carrera. Historical Review of Zig-Zag Theories for Multilayered Plates and Shells. *Appl. Mech. Rev.*, **56**, 287-308, (2003).
- [10] D.J. Chen, D.K. Shah and W.S. Chan. Interfacial Stress Estimation Using Least-square Extrapolation and Local Stress Smoothing in Laminated Composites. *Computers and Structures*, **58**, 765-774, (1996).
- [11] E.N. Dvorkin and K.J. Bathe. A Continuum Mechanics Based Four-node Shell Element for General Nonlinear Analysis. *Engineering and Computations*, **1**, 77-88, (1984).

- [12] P. Foraboschi. Behavior and Failure Strength of Laminated Glass Beams. *Journal of Engineering Mechanics*, **133**, 12, 1290-1301, (2007).
- [13] M. Fröling and K. Persson. Application of Solid-shell Elements to Laminated Glass Structures. *Proceedings of the XXIV A.T.I.V. International Conference/ 59th NGF Annual Meeting*, July 9-10 2009, Parma, Italy.
- [14] M. Haldimann, A. Luible and M. Overend. *Structural Use of Glass*. Structural Engineering Documents, 10. IABSE, Zürich, (2008).
- [15] M. Harnau and K. Schweizerhof. About Linear and Quadratic "Solid-Shell" Elements at Large Deformations. *Computers and Structures*, **80**, 805-817, (2002).
- [16] R. Hauptmann and K. Schweizerhof. A Systematic Development of 'Solid-shell' Element Formulations for Linear and Nonlinear Analyses Employing Only Displacement Degrees of Freedom. *International Journal for Numerical Methods in Engineering*, **42**, 49-69, (1998).
- [17] R. Hauptmann, K. Schweizerhof and S. Doll. Extension of the 'Solid-shell' Concept for Application to Large Elastic and Large Elastoplastic Deformations. *International Journal for Numerical Methods in Engineering*, **49**, 1121-1141, (2000).
- [18] T.J.R. Hughes. *The Finite Element Method: Linear Static and Dynamic Finite Element Analysis*. Dover Editions, New Jersey, Second edition, (2000).
- [19] P. Krawczyk. Nonlinear Analysis of Layered Structures with Weak Interfaces, PhD thesis, École Polytechnique Fédérale de Lausanne, (2006).
- [20] O. Larsson. *Shear Capacity in Adhesive Glass-joints*. Master's thesis, Lund University of Technology, (2008).
- [21] K.P. Li and S. Cescotto. An 8-node Brick Element with Mixed Formulation for Large Deformation Analyses. *Computer Methods in Applied Mechanics and Engineering*, **141**, 157-204, (1997).
- [22] W.K. Liu, Y. Guo, S. Tang and T. Belytschko. A Multiple-quadrature Eight-node Hexahedral Finite Element for Large Deformation Elastoplastic Analysis. *Computer Methods in Applied Mechanics and Engineering*, **154**, 69-132, (1998).
- [23] J. Malmberg. *A Finite Element Based Design Tool for Point Fixed Laminated Glass*. Master's thesis, Lund University of Technology, (2006).
- [24] H. Parish. A Continuum-based Shell Theory for Non-linear Applications. *International Journal for Numerical Methods in Engineering*, **38**, 1855-1883, (1995).
- [25] J.N. Reddy. *Mechanics of Laminated Composite Plates. Theory and Analysis*. CRC Press, Boca Raton, (1997).
- [26] J.C. Simo and M.S. Rifai. A Class of Mixed Assumed Strain Methods and the Method of Incompatible Modes. *International Journal for Numerical Methods in Engineering*, **29**, 1595-1638, (1990).
- [27] B. Weller and T. Schadow. Designing of Bonded Joints in Glass Structures. *Proceedings of the 10th Glass Performance Days*, June 15-18 2007, Tampere, Finland.

Paper 3

DESIGNING BOLT FIXED LAMINATED GLASS WITH STRESS CONCENTRATION FACTORS

MARIA FRÖLING AND KENT PERSSON

Designing Bolt Fixed Laminated Glass with Stress Concentration Factors

Maria Fröling and Kent Persson

Abstract

A method for determining stress concentration factors for laminated glass balustrades with 2+2 bolt fixings is developed. The stress concentration factors are presented graphically in design charts. Through the use of simple formulas and the design charts, the maximum principal stresses of the balustrade can be determined for an arbitrary combination of the geometry parameters involved.

1 Introduction

Recently, demand from architects has made it more common to use glass as a structural material. Unfortunately, knowledge about mechanical properties of glass is less than for other structural materials and there is a lack of guidelines on how to perform strength design of glass structures. Thus, there is a risk for inaccurate predictions of glass strength which may result in sudden failures due to the brittle nature of the material glass. In order to increase safety of glass constructions, laminated glass may be used instead of single layered glass. Laminated glass consists of two or more glass layers with intermediate PVB (polyvinylbutyral) layers. Laminated glass displays a complicated structural mechanical behavior due to the combination of a very stiff material (glass) and a very soft material (PVB), [1]. When a laminated glass structure is subjected to certain loads and boundary conditions, discontinuous stress distributions may develop, ([2], [11]). The discontinuities are most pronounced around holes and edges, that is, in the regions where the largest stress concentrations often occur. It is of significant importance that these stress concentrations are accurately determined. Accurate glass strength prediction is also of advantage from the perspective of using material efficiently.

Design of glass structures can be performed using tables and graphs contained in design standards as far as common geometries and loading conditions are concerned. For more complicated geometries and support conditions, for instance bolt fixings, a more detailed computational analysis is often required, [7]. The traditional method for predicting stress distributions in laminated glass structures with bolt fixings is to use three dimensional models in finite element analyses. The large models that are required for accurate stress predictions, make this type of analyses practically impossible from a computational perspective. Apparently, there is a need for strength design methods with scientific and technical base for laminated glass structures with bolt fixings.

In previous work, the authors implemented a solid-shell element, [3], suitable for stress predictions of large laminated glass structures with many bolt fixings, [6]. The computational efficiency is increased while the accuracy of the stress predictions is preserved.

However, the use of this method requires advanced knowledge of finite element analysis. In the present work, the solid-shell element is used in finite element analysis in order to develop a method for determining stress concentration factors for laminated glass balustrades with 2 + 2 bolt fixings. With the use of the stress concentration factors, the maximum of the largest principal stress of the balustrade can be determined for arbitrary geometrical parameter combinations. The computed stress values could be used in strength design of the balustrade.

Design methods in terms of formulas, tables or graphs are particularly rare when it comes to bolt fixed laminated glass design. A comprehensive overview of the current state of knowledge is given in [7]. Existing design methods for vertical bolt fixed glass are typically constructed for the case of a uniformly distributed wind load and fixed positions of the bolts. In this work, simple formulas and charts are developed for balustrades subjected to a uniform line load and with variable positions of the bolt fixings. The aim is to make the design of bolt fixed laminated glass balustrades possible without performing high level mathematics or advanced finite element analysis.

2 Available Methods for Stress Prediction of Bolt Fixed Laminated Glass

Currently, few studies are available that describe guidelines or methods for stress prediction of bolt fixed laminated glass. In [12], a single glass pane with one bolt fixing is investigated. The pane is subjected to in-plane load. For stress predictions, a finite element analysis is performed. A novelty is that a procedure for verification of the finite element model is developed. This procedure is of advantage, because it serves to standardize the required finite element analyses so that a designer less experienced with finite element analysis can obtain reliable results. As mentioned previously, [7] provides an excellent overview on how to deal with glass in its role as a structural material. In the book, an example of a design chart for bolt fixed laminated glass is presented. The dimensions of the glass panes can be selected given the position of the bolts, the design strength and a specific value of the load. The load type is a uniformly distributed wind load. In [13], guidelines for structural analyses of glass panels subjected to in-plane shear forces are given. The analyses are performed by means of the finite element method. The guidelines are valid for linear supported as well as point fixed glass panes. [14] presents experimental and numerical investigations of small-scaled axially compressed laminated glass panels that are point fixed. A comprehensive stress analysis is made, a parametric study is performed and an empirical formula for the stress concentration factor is derived. [11] deals with the development of a design program for bolt fixed laminated glass facades and balustrades. The program aims to facilitate design of those glass structures and the user does not need to have any knowledge about the finite element method.

Many of the existing stress prediction methods for laminated glass design contain recommendations on how to perform finite element analyses. That means that the designer or analyst has to be very familiar with the finite element method. One major aim of this work is to present a method that does not require knowledge of neither finite element

analysis nor advanced mathematics. Overall, few stress prediction methods exist for laminated glass structures with bolt fixings, and for this particular case of laminated glass balustrades with four bolt fixings with non-fixed positions, only the work of [11] exists. As a complement to that work, this paper develops simple formulas and charts that can be used for stress prediction of bolt fixed laminated glass balustrades.

3 Design of Bolt-fixed Balustrade Glass with Stress Concentration Factors

In this paper, a method is developed for determining stress concentration factors, α , for bolt fixed laminated glass balustrades. α relates the nominal stress value, σ_{Nom} , to the maximum (positive) principal stress value, σ . σ typically occurs in the vicinity of a hole. σ_{Nom} is defined as the maximum (positive) principal stress for the case of a laminated glass structure of the same dimensions as the balustrade, but without holes. However, the influence of the reaction forces at the bolt locations are included in the computation.

When σ_{Nom} has been determined, the case of a balustrade with bolt fixings can be considered. It remains to find the stress concentration factor α as $\sigma = \alpha\sigma_{Nom}$, where σ is the maximum (positive) principal stress of the balustrade. σ occurs at the edge of a bore hole. This problem is too complicated to be treated analytically. A later section deals with the finite element modelling of a balustrade with 2+2 bolt fixings. With the aid of the finite element model, design charts are developed so that the stress concentration factors, α , can be determined for arbitrary parameter combinations.

4 Stresses in a Laminated Glass without Holes

A laminated glass without holes subjected to three-point bending can be modelled as a simply supported beam that is subjected to a bending moment, given that the load and boundary conditions are symmetric. The maximum principal stresses for a laminated beam that is subjected to a bending moment may be determined analytically, [4]. The stresses are derived for a laminated glass beam consisting of two glass layers with an interlayer of PVB. Figure 1 shows the geometry of the beam model applied to a balustrade.

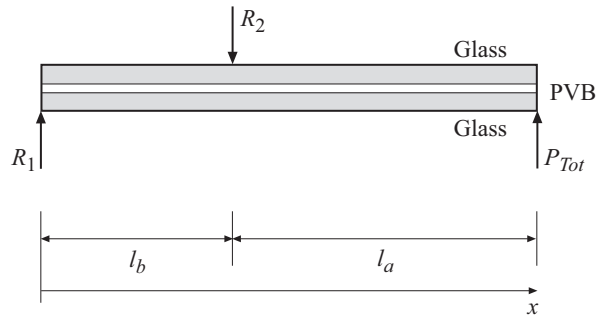


Figure 1: Geometry of beam model.

According to Swedish construction standards, the balustrade is subjected to a uniformly distributed line load, P , at the top of the balustrade in the direction normal to the glass pane. The load conditions are displayed in Figure 2.

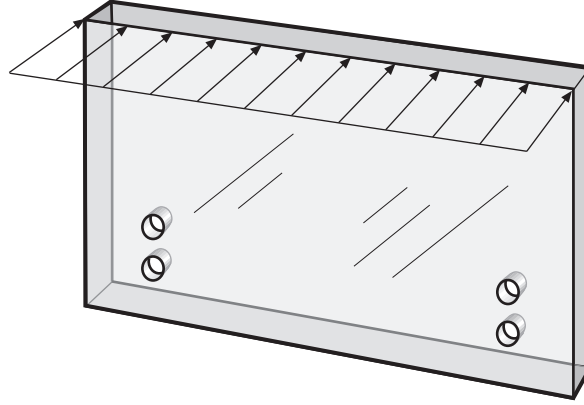


Figure 2: Description of load conditions.

Multiplying the line load, P , with the width, w , of the glass pane gives the total load, P_{Tot} . R_1 and R_2 are reaction forces that represent the bolt locations. The reaction force R_2 and the moment, $M(x)$, can be derived by equilibrium equations as

$$R_2 = P_{Tot} \left(1 + \frac{l_a}{l_b}\right) \quad \text{and} \quad M(x) = \frac{R_2 l_a x}{(l_a + l_b)}. \quad (1)$$

The moment equation is valid on the interval $0 \leq x \leq l_b$. In [4], a differential equation that governs the behavior of the laminated beam problem is derived. As a starting point for the derivation, an infinitesimal beam element is considered. The forces and displacements of the beam element is shown in Figure 3.

As a starting point, the displacement between the individual glass panes, $u_s(x)$, is given by

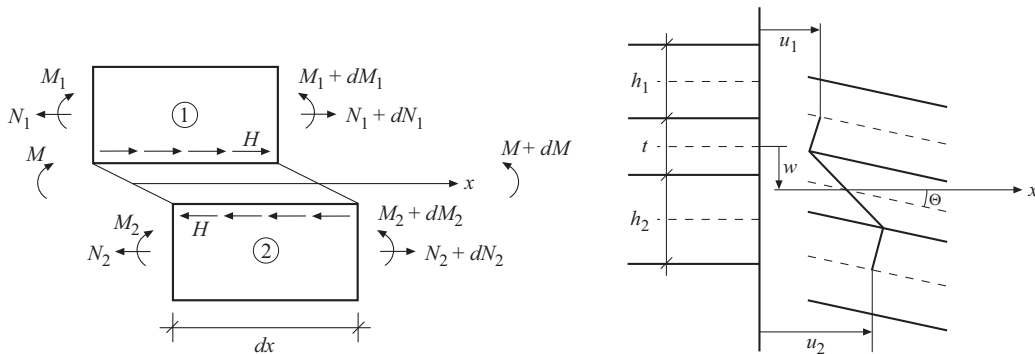


Figure 3: Forces acting on an infinitesimal laminated beam element, to the left and displacements to the right.

$$u_s(x) = u_2(x) - u_1(x). \quad (2)$$

Derivating (2) with respect to x gives

$$\frac{d}{dx}u_s = \frac{d}{dx}u_2 - \frac{d}{dx}u_1. \quad (3)$$

The normal strain components in the x -direction are defined to be the derivatives of the corresponding displacement components, which means that (3) can be written as

$$\frac{d}{dx}u_s = \varepsilon_2 - \varepsilon_1. \quad (4)$$

ε_1 is the normal strain in the x -direction of the upper glass pane, in the lowermost fibre of that pane. ε_2 is the normal strain in the x -direction of the lower glass pane, in the uppermost fibre of that glass pane.

For one single pane, Navier's formula, [8], of the form

$$\sigma = \frac{M}{I}y + \frac{N}{A}. \quad (5)$$

gives the total normal stress in the x -direction, σ . Since the small deformation assumption prevails, Hooke's law $\sigma = E\varepsilon$ applies and equation (5) then yield the normal strain in the x direction, ε , for each glass layer as

$$\varepsilon_1 = \frac{M_1}{EI_1} \frac{h_1}{2} + \frac{N_1}{EA_1} \quad \text{and} \quad \varepsilon_2 = \frac{-M_2}{EI_2} \frac{h_2}{2} + \frac{N_2}{EA_2}, \quad (6)$$

where h_1 and h_2 are the thicknesses of glass panes one and two respectively.

Substituting equations (6) into (3) gives

$$\frac{du_s}{dx} = -\frac{M_2}{EI_2} \frac{h_2}{2} - \frac{M_1}{EI_1} \frac{h_1}{2} + \frac{N_2}{EI_2} - \frac{N_1}{EI_1}. \quad (7)$$

The equation to describe the deformation of a basic beam cross section, which due to the kinematic assumptions made can be applied as

$$\frac{d^2w}{dx^2} = -\frac{M_1}{EI_1} = -\frac{M_2}{EI_2}, \quad (8)$$

where $w(x)$ is the beam deformation (in the y direction). From horizontal equilibrium of a single beam cross section, $N_1(x) = -N_2(x) = N(x)$ is given and equation (7) can be written as

$$\frac{du_s}{dx} = \frac{d^2w}{dx^2} h_t - N \left(\frac{1}{EA_1} + \frac{1}{EA_2} \right), \quad (9)$$

where $h_t = \frac{h_1}{2} + \frac{h_2}{2}$.

It is assumed that the shear deformation, u_s , of the PVB layer is given by

$$u_s(x) = \gamma h_{PVB} = \frac{H t_{PVB}}{G_{PVB} l_w} = \frac{H}{k_{PVB}}, \quad (10)$$

where γ is the shear strain, $k_{PVB} = \frac{G_{PVB}l_w}{t_{PVB}}$ is the spring stiffness, G_{PVB} is the shear modulus, l_w the width and t_{PVB} is the thickness of the PVB layer.

From horizontal equilibrium of the first glass pane,

$$H(x) = -\frac{dN}{dx}. \quad (11)$$

Equations (10) and (11) are inserted into (9) which yields

$$-\frac{d^2N}{dx^2} \frac{1}{k_{PVB}} = \frac{d^2}{dx^2} v h_t - N \left(\frac{1}{EA_1} + \frac{1}{EA_2} \right). \quad (12)$$

A moment equilibrium computation about the left part of the beam cross section at the center of gravity of the second glass pane gives

$$M = M_1 + M_2 - N h_t. \quad (13)$$

Equations (13) and (8) together gives

$$\frac{d^2w}{dx^2} = -\frac{M}{EI_1 + EI_2} - \frac{N h_t}{EI_1 + EI_2}. \quad (14)$$

Combining equations (14) and (12) yields the governing differential equation for the problem

$$\frac{d^2}{dx^2} N(x) - c_2 N(x) = c_1 M(x) \quad (15)$$

where the following constants are defined in order to simplify the equation

$$c_1 = k_{PVB} \frac{h_t}{E_g I_1 + E_g I_2} \quad \text{and} \quad c_2 = k_{PVB} \left(\frac{1}{E_g A_1} + \frac{1}{E_g A_2} + \frac{h_t^2}{E_g I_1 + E_g I_2} \right). \quad (16)$$

where E_g is the modulus of elasticity for glass, I_1 is the moment of inertia of a cross section of the upper glass pane, I_2 is the moment of inertia of a cross section of the lower glass pane, A_1 is the cross section area of the upper glass pane, A_2 is the cross section area of the lower glass pane, and t_g is the glass pane thickness. For the balustrades considered, it is assumed that the glass panes have equal cross section geometries, and thus $I_1 = I_2 = I$, $h_1 = h_2 = t_g$ and $A_1 = A_2 = A$ are used in the following.

The homogeneous and particular solution, respectively to (15) is given by

$$N(x) = B \sinh(\sqrt{c_2}x) + C \cosh(\sqrt{c_2}x) - \frac{c_1 R_2 l_a x}{c_2 (l_a + l_b)}. \quad (17)$$

To determine the constants B and C the boundary conditions $N(0) = 0$ and $\left(\frac{dN}{dx}\right)_{x=l_b} = 0$ yields $C = 0$ and

$$B = \frac{c_1 R_2 l_a}{c_2 \sqrt{c_2} (l_a + l_b) \cosh(\sqrt{c_2} l_b)}. \quad (18)$$

The final solution may be written as

$$N(x) = \frac{c_1 R_2 l_a}{c_2 \sqrt{c_2} (l_a + l_b) \cosh(\sqrt{c_2} l_b)} \sinh(\sqrt{c_2} x) - \frac{c_1 R_2 l_a x}{c_2 (l_a + l_b)}. \quad (19)$$

Since $M_1(x) = M_2(x)$ equation (13) can be written

$$M_1(x) = M_2(x) = \frac{1}{2}(M(x) + h_t N(x)). \quad (20)$$

From Navier's formula, (5), the normal stress in the x-direction of one glass pane can be computed. The maximum tensile stress occurs at the lower surface of the laminate. Since the shear stresses are zero at the surfaces of the laminate, the tensile stress in the x-direction at the lower surface of the laminate is equal to the maximum (positive) principal stress. σ_{Nom} is defined as the maximum (positive) principal stress (evaluated at $x = l_b$). At the lower surface of the laminate, $M_2(x) = M(x)$, $I_2 = I$, $N_2(x) = -N_1(x) = -N(x)$ and $y = -\frac{t_g}{2}$. Thus,

$$\sigma_{Nom} = \frac{M(l_b)}{\frac{wt_g^2}{6}} - \frac{N(l_b)}{wt_g}. \quad (21)$$

Note that equation (21) is valid for glass panes with rectangular cross sections only. For the balustrades considered in this paper, this will always be the case.

5 Determining Stress for a Bolt Fixed Balustrade

In this section, a finite element model is developed with the purpose of determining the stresses in a point fixed balustrade glass. The finite element model yields a value for the largest maximum principal stress of the balustrade for an arbitrary parameter combination. In previous sections, this quantity is denoted σ . The goal is to determine the stress concentration factor, α , for each parameter combination. This is achieved through determining both σ_{Nom} and σ for all possible parameter combinations and then compute the corresponding values of α . Later, α is represented in simple design charts so that for each parameter combination, the value of α can be determined from the charts.

The in-plane geometry of the balustrade is displayed in Figure 4. In the figure, the parameters that determine the basic in-plane geometry of the glass pane are displayed. The bore hole has the diameter d_h and the bolt head has the diameter d_b . It is convenient to construct design charts for each glass pane thickness, t_g , separately. The height of the balustrade, l_a , and the vertical position of the bolts, l_c , are set to $l_a = 1.25$ m and $l_c = 0.24$ m. It should be noted that the edge distance, a_w , is equal for all four bolt holes.

Table 1 summarizes the relevant geometry parameters. The ranges over which every variable parameter is allowed to vary are also given. A standard value $t_{PVB} = 0.76$ mm is used for the thickness of the PVB layer. In the finite element model, only the EPDM bush between the bolt head and the glass pane is included and its thickness is fixed to $t_{EPDM} = 3$ mm.

The material parameters used are $E_g = 78$ GPa, $\nu_g = 0.3$, $E_{PVB} = 6$ MPa, $\nu_{PVB} = 0.43$, $E_{EPDM} = 20$ MPa, and $\nu_{EPDM} = 0.45$.

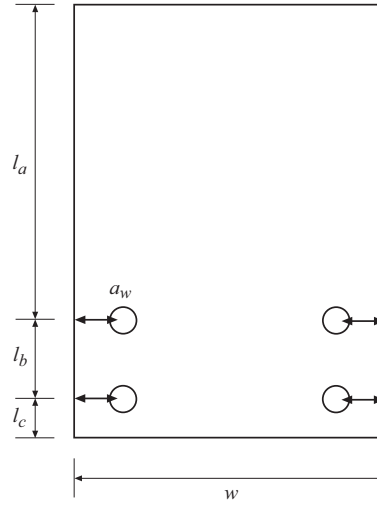


Figure 4: Geometry of balustrade.

Table 1: List of geometry parameters.

Parameter	Value
l_a	1.25 m
l_c	0.24 m
t_{PVB}	0.76 mm
t_{EPDM}	3 mm
l_b	0.2, 0.4, 0.8 m
a_w	$0.1 - (\frac{w}{2} - 0.1)$ in step of 0.025
w	0.9-2.7 m in step of 0.3 m
d_h	15-40 mm in step of 5 mm
t_g	6, 8, 10, 12 mm
d_b	60 mm

The complex geometry of the balustrade requires the use of a mesh generator. The solid-shell element, [3], used has quadrilateral in-plane geometry and therefore a quadrilateral mesh generator is used. In the finite element analysis, the mesh generator and finite element program of [5] and [9] are used together with Matlab. Due to symmetry, only half of the balustrade needs to be modeled. Along the symmetry line, displacements in the in-plane direction normal to the symmetry line are set to zero.

When computing α , a value of the line load P is arbitrary but is in the simulations set to the value $P = 3$ kN/m. When the charts are constructed, α can be determined irrespective of design load by use of the available charts.

When modeling the bolts, only the EPDM bushes are included in the model. The bushes are modeled by means of a spring model, where springs are connected, in all three coordinate directions, to the nodes that are located on the contact surfaces between bush and glass. In the direction normal to the balustrade, springs with stiffness

$$k = \frac{E_{EPDM}\Delta A}{t_{EPDM}} \quad (22)$$

are connected, [15]. ΔA is the influence area of each node, determined by

$$\Delta A = \int_A \mathbf{N}^T dA. \quad (23)$$

\mathbf{N} is the global shape function vector, [5]. Equivalently, for the other coordinate directions shear springs with stiffness

$$k_s = \frac{G_{EPDM}\Delta A}{t_{EPDM}} \quad (24)$$

are used, [10]. The springs are fixed to their surrounding, which means that the corresponding displacements are set to zero. The spring stiffnesses, k_i , are thus assembled into the global stiffness matrix, \mathbf{K} , according to

$$\mathbf{K}_{ii} = \mathbf{K}_{ii} + k_i. \quad (25)$$

k_i represents the spring stiffness corresponding to degree of freedom i . The bushes are modeled explicitly only for the sides of the laminate where the reaction forces are acting on the glass. These positions are indicated in Figure 1. On the other sides of the laminate, the bolts are not modelled.

When meshing the structure, a two dimensional mesh of the geometry illustrated in Figure 4 is first created. To form a three-dimensional mesh, this mesh is swept in the direction normal to the two dimensional structure. A special feature of the solid-shell element, [3], only one element per material layer is required to reach a good solution.

6 Design Charts for Determination of Stress Concentration Factors

The process of determining σ by means of the finite element method described in the previous section is time consuming and requires decent knowledge about the finite element method. In order for the glass designer to avoid using the finite element method, a simplified method for determining σ for arbitrary combinations of certain design parameters is suggested. The method contains graphical representations, design charts, that allow α to be determined for a certain parameter combination. When σ_{Nom} is determined for the same parameters, σ is practically known. The required equations for determination of σ_{Nom} are (1), (19), (20) and (21).

One design chart is made for each possible combination of glass thickness, t_g , glass pane width, w , bolt head diameter, d_b , and bore hole diameter, d_h . As examples, design charts for the parameter combination [$w = 0.9$ m, $d_b = 60$ mm, $d_h = 15$ mm] with [$t_g = 6, 8, 10, 12$] mm are shown in Figures 5-8.

The suggested method for determining σ by use of the design charts starts with computing σ_{Nom} for an arbitrary combination of the parameters t_g , w and l_b . The design chart for the

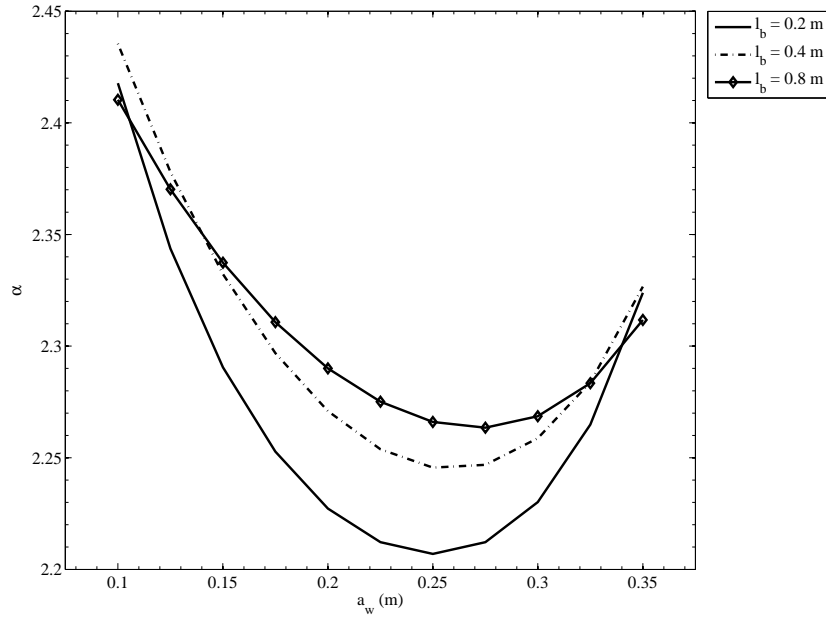


Figure 5: Design chart for $t_g = 6$ mm, $w = 0.9$ m, $d_b = 60$ mm and $d_h = 15$ mm.

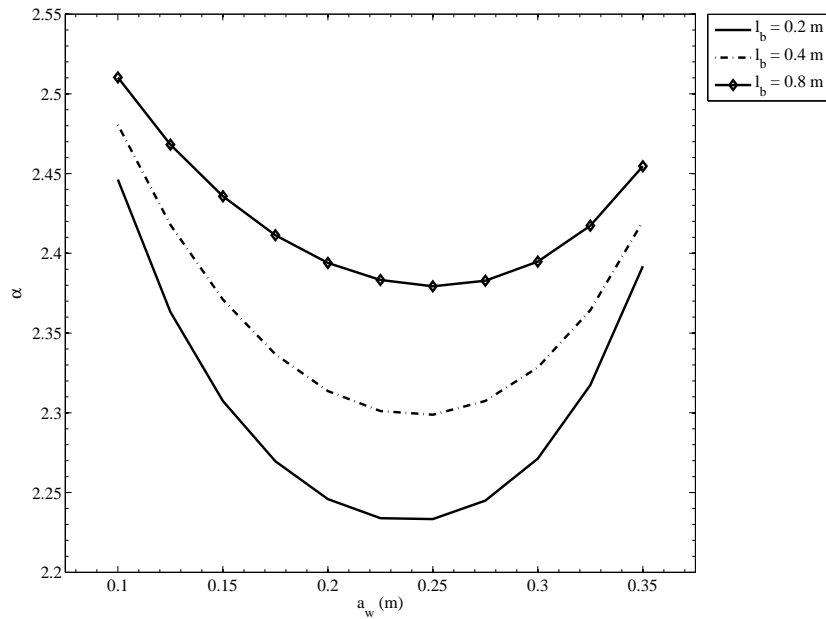


Figure 6: Design chart for $t_g = 8$ mm, $w = 0.9$ m, $d_b = 60$ mm and $d_h = 15$ mm.

selected values of (t_g, w) is then consulted. Remembering that a value of l_b has already been selected, the isoline corresponding to the value of this parameter is chosen in the design chart. It remains to choose a value of a_w and read off a corresponding value of the stress concentration factor, α , from the design chart. Using the relation $\sigma = \alpha \sigma_{Nom}$, σ is

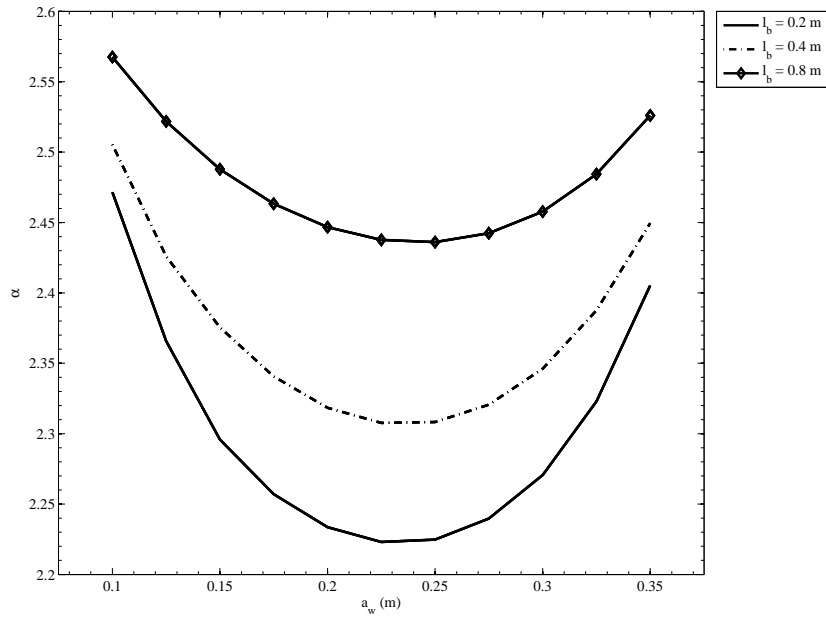


Figure 7: Design chart for $t_g = 10$ mm, $w = 0.9$ m, $d_b = 60$ mm and $d_h = 15$ mm.

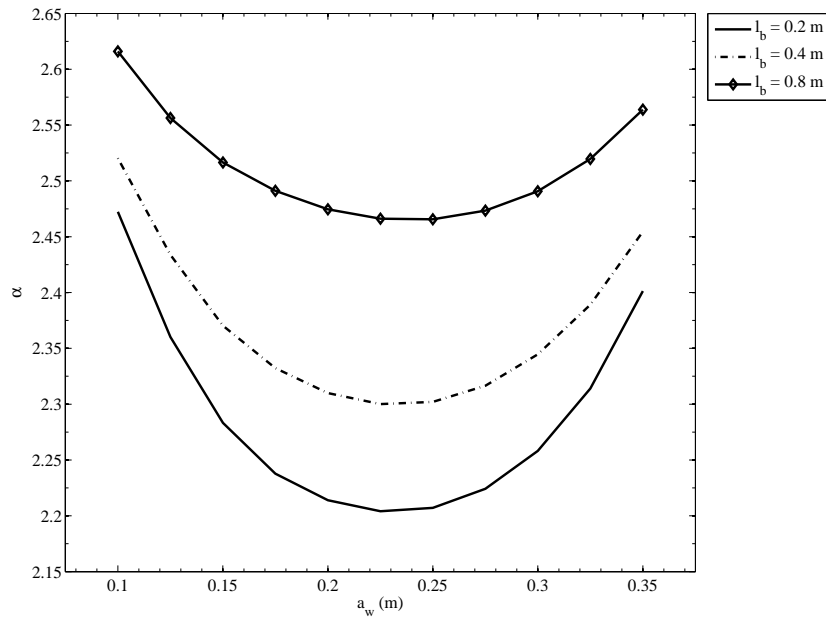


Figure 8: Design chart for $t_g = 12$ mm, $w = 0.9$ m, $d_b = 60$ mm and $d_h = 15$ mm.

determined. σ is the maximum (positive) principal stress value in the balustrade and this value is compared to a fracture criterion. If the fracture criterion is met, the parameter combination is possible. If the value of σ fails to meet the fracture criterion, at least one parameter value has to be changed and the procedure to determine σ starts over again.

The optimal positions of the bolts may be determined directly from the design charts. Since the lowest value of α gives the lowest stresses at the bolts, the charts directly provide this information.

7 Conclusions

A method for the determination of stress concentration factors has been developed for two ply laminated glass balustrades with 2 + 2 bolt fixings. Using the method, the designer can determine the maximum (positive) principal stress value for each combination of glass ply thickness, width of the glass pane, bolt position, bolt head diameter and bore hole diameter using simple formulas and charts, and thus avoiding advanced and computationally expensive finite element analysis.

References

- [1] M.Z. Aık and S. Tezcan. A Mathematical Model for the Behavior of Laminated Glass Beams. *Computers and Structures*, **83**, 1742-1753, (2005).
- [2] C. Bength. *Bolt Fixings in Toughened Glass*. Master's thesis, Lund University of Technology, (2005).
- [3] R.P.R. Cardoso, J.W. Yoon, M. Mahardika, S. Choudhry, R.J. Alves de Sousa and R.A. Fontes Valente. Enhanced Assumed Strain (EAS) and Assumed Natural Strain (ANS) Methods for One-point Quadrature Solid-shell Elements. *International Journal for Numerical Methods in Engineering*, **75**, 156-187, (2008).
- [4] C. Carrick and J. Vasur. *Styvhet och Hållfasthet hos Laminerat Glas*. Master's thesis, Royal Institute of Technology, (2002).
- [5] O. Dahlblom et al. *CALFEM-A Finite Element Toolbox to MATLAB*. Division of Structural Mechanics Report TVSM 9001, Lund University of Technology, (1999).
- [6] M. Fröling and K. Persson. Application of Solid-shell Elements to Laminated Glass Structures. *Proceedings of the XXIV A.T.I.V. Conference/59th NGF Annual Meeting*, July 9-10 2009, Parma, Italy.
- [7] M. Haldimann, A. Luible and M. Overend. *Structural Use of Glass*. Structural Engineering Documents, 10. IABSE, Zürich, (2008).
- [8] S. Heyden, O. Dahlblom, A. Olsson and G. Sandberg. *Introduktion till Strukturmekaniken*. Studentlitteratur, (2008).
- [9] J. Lorentzon. *CALFEM Meshing Module*. Division of Structural Mechanics and Division of Solid Mechanics, Lund University of Technology, (2010).
- [10] M.R. Maheri and R.D. Adams. Determination of Dynamic Shear Modulus of Structural Adhesives in Thick Adherend Shear Test Specimens. *International Journal of Adhesion and Adhesives*, **22**, 119-127, (2002).

- [11] J. Malmborg. *A Finite Element Based Design Tool for Point Fixed Laminated Glass*. Master's thesis, Lund University of Technology, (2006).
- [12] I. Maniatis. *Numerical and Experimental Investigations on the Stress Distribution of Bolted Glass Connections under In-plane Loads*. Doctoral thesis, Technische Universität München, (2006).
- [13] D. Mocibob. *Glass Panel under Shear Loading - Use of Glass Envelopes in Building Stabilization*. Doctoral thesis, École Polytechnique Fédérale de Lausanne, (2008).
- [14] D. Mocibob and J. Belis. Coupled Experimental and Numerical Investigation of Structural Glass Panels with Small Slenderness Subjected to Locally Introduced Axial Compression. *Engineering Structures*, **32**, 753-761, (2010).
- [15] N.S. Ottosen and H. Petersson. *Introduction to the Finite Element Method*. 2nd Ed. Division of Structural Mechanics Report TVSM 3014, Lund University of Technology, (1991).
- [16] D.G. Zill and M.R. Cullen. *Differential Equations with Boundary-Value Problems*. 4th Ed. International Thomson Publishing Inc., (1997).